Characterization of Bipolar Disorder Patient-Specific Induced Pluripotent Stem Cells from a Family Reveals Neurodevelopmental and mRNA Expression Abnormalities

The Harvard community has made this article openly available. **Please share** how this access benefits you. Your story matters

Characterization of Bipolar Disorder Patient-Specific Induced Pluripotent Stem Cells from a Family Reveals Neurodevelopmental and mRNA Expression Abnormalities

Jon M. Madison[1,2,3,#,*], **Fen Zhou**[1,2,*], **Aparna Nigam**[1,3], **Ali Hussain**[1,2], **Douglas D. Barker**[1], **Ralda Nehme**[1,4,7], **Karlijn van der Ven**[2], **Jenny Hsu**[1,2], **Pavlina Wolf**[1,2,7], **Morgan Fleishman**[1,2], **Colm O'Dushlaine**[1], **Sam Rose**[1], **Kimberly Chambert**[1], **Frank H. Lau**[4], **Tim Ahfeldt**[4], **Erroll H. Rueckert**[1,2,8], **Steven D. Sheridan**[8], **Daniel M. Fass**[1,7,8], **James Nemesh**[1,6], **Thomas E. Mullen**[1,6], **Laurence Daheron**[4], **Steve McCarroll**[1,6], **Pamela Sklar**[5], **Roy H. Perlis**[1,2,3,8], and **Stephen J. Haggarty**[1,2,3,7,8,#]

[1]Stanley Center for Psychiatric Research, Broad Institute of MIT & Harvard, Cambridge, MA 02142, USA

[2]Psychiatric & Neurodevelopmental Genetics Unit, Center for Human Genetics Research, Massachusetts General Hospital, Boston, MA 02114, USA

[3]Department of Psychiatry, Massachusetts General Hospital, Boston, MA 02114, USA

[4]Department of Stem Cell & Regenerative Biology, Harvard University, Cambridge, MA

[5]Department of Psychiatry, Mount Sinai School of Medicine, New York, NY 10029, USA

[6]Department of Genetics, Harvard Medical School, Boston, MA 02115, USA

[7]Department of Neurology, Massachusetts General Hospital & Harvard Medical School, Boston, MA 02114, USA

[8]Chemical Neurobiology Laboratory, Center for Human Genetic Research, Massachusetts General Hospital, Boston, MA 02114, USA

Abstract

Bipolar disorder (BD) is a common neuropsychiatric disorder characterized by chronic recurrent episodes of depression and mania. Despite evidence for high heritability of BD, little is known about its underlying pathophysiology. To develop new tools for investigating the molecular and cellular basis of BD we applied a family-based paradigm to derive and characterize a set of 12 induced pluripotent stem cell (iPSC) lines from a quartet consisting of two BD-affected brothers and their two unaffected parents. Initially, no significant phenotypic differences were observed between iPSCs derived from the different family members. However, upon directed neural differentiation we observed that CXCR4 (CXC chemokine receptor-4) expressing central nervous system (CNS) neural progenitor cells (NPCs) from both BD patients compared to their unaffected

[#]Correspondence: jmadison@broadinstitute.org (JM), shaggarty@mgh.harvard.edu (SJH).
[*]These authors contributed equally

parents exhibited multiple phenotypic differences at the level of neurogenesis and expression of genes critical for neuroplasticity, including WNT pathway components and ion channel subunits. Treatment of the CXCR4+ NPCs with a pharmacological inhibitor of glycogen synthase kinase 3 (GSK3), a known regulator of WNT signaling, was found to rescue a progenitor proliferation deficit in the BD-patient NPCs. Taken together, these studies provide new cellular tools for dissecting the pathophysiology of BD and evidence for dysregulation of key pathways involved in neurodevelopment and neuroplasticity. Future generation of additional iPSCs following a family-based paradigm for modeling complex neuropsychiatric disorders in conjunction with in-depth phenotyping holds promise for providing insights into the pathophysiological substrates of BD and is likely to inform the development of targeted therapeutics for its treatment and ideally prevention.

Keywords

bipolar disorder; stem cell; iPSC; neurodevelopment; corticogenesis; neuroplasticity; calcium channels; ion channels; lithium; GSK3

INTRODUCTION

The precise relationship between the etiology and cellular pathophysiology of bipolar disorder (BD) remains poorly understood[1–3]. In light of its high heritability[4,5], genome-wide association studies (GWAS) have been used to identify genes and pathways associated with BD risk. Several GWAS and their meta-analyses have reported several genomic loci that meet the criteria of genome-wide significance[5–7]. However, despite these genetic efforts the biological basis of BD remains elusive and the path toward highly effective, disease-modifying, targeted therapeutics is uncertain. Measurable brain pathology has had limited success as well; consistent neuroanatomical deficits have been difficult to identify. Some of the most consistent imaging results have implicated grey matter changes in both emotion and reward processing circuits[8]. Anatomical deficits such as these brain volume changes have prompted some researchers to label BD a "neurodevelopmental" disorder, but the basis for such neurodevelopmental deficits has remained unclear. Other data that supports such a model implicate neural stem cell or neural progenitors. For instance, mutations in the DISC1 gene have been associated with several forms of mental illness in an extended Scottish pedigree[9], including BD[10]. DISC1 has been shown to regulate neural progenitor proliferation through inhibition of GSK3μ[11], a known target of the mood stabilizer lithium signaling[12–14]. Furthermore antidepressant treatments have been shown to alter neural stem neurogenesis and plasticity. Thus, with what is proving to be a highly complex genetic landscape, modeling approaches investigating changes in single or small numbers of genes are incapable of capturing the full spectrum of factors that may impact pathophysiological process relevant to BD.

In light of the need to examine genetically associated loci across a developmental continuum, and implication of neural stem cell neurogenesis in mood regulation, cellular models that allow access to different developmental stages would be invaluable to the further study of mood disorders. Fortunately, recent advances in human stem-cell biology

now provide the technology to create genetically accurate, patient-derived cellular tools through the reprogramming of somatic cells to a pluripotent state. Multiple central nervous system (CNS) lineages, including neurons and glia, can be derived from iPSCs facilitating access to *ex vivo* characterization of patient-specific, cellular phenotypes that have otherwise been inaccessible[15–17]. Reflective of the increasing value of this strategy for human disease modeling, disease-specific, stem cell models have now been generated from multiple monogenic disorders using somatic cell reprogramming[18–24]. However, despite the potential for providing a basic human cellular model system and critically needed insight into the underlying pathophysiology, to date, only limited application of iPSC modeling has been performed in the context of complex genetic disorders[25–28].

In the case of BD, recent analysis of common genetic variation associated with BD susceptibility using powerful genome-wide approaches, has confirmed that BD is highly polygenic in nature with the suggestion that there may be many thousands of common variants that contribute small or modest levels of risk for BD[6]. Thus, for modeling of BD with iPSCs choosing individuals at random would make it difficult to identify individuals, affected or unaffected, that do not harbor risk alleles, especially common variants associated with the disease, and the selection of a genetically appropriate control is problematic. Moreover, randomly selected BD patients might also be expected to harbor variants that only modestly affect cellular phenotypes in cellular models. Alternatively, consideration of family history and the number of risk alleles an individual might harbor (i.e. the genetic load) when selecting individuals for reprogramming may allow one to select individuals from a pedigree enriched for BD in order to enrich for deleterious alleles. Following this rationale, the more psychiatric disease in the family the higher the genetic risk of any individual will be, and thus the greater the potential for enrichment of deleterious alleles and potentially observable *in vitro* cellular phenotypes. Furthermore, exploitation of familial relationships as part of iPSC model characterization enables the explicit prediction that the affected individuals will exhibit phenotypes not found in the unaffected family members. This prediction should become increasingly powerful for delineating true disease-specific phenotypes from patient-specific phenotypes as size of the family increases.

To begin to explore the potential utility of such a family-based paradigm for iPSC-based modeling of BD, which to date has not been applied to any human genetic disorder, here we generated and characterized 12 iPSC lines from a family with two unaffected parents and two BD male offspring. Overall, while no significant differences were observed between the 12 iPSCs, upon directed differentiation to the neural lineage our studies revealed several neurodevelopmental phenotypes in both BD-patient cells compared to the phenotypes of their unaffected parents. Additionally, specific defects in the expression of genes important for neurogenesis and neuroplasticity were observed, thereby pointing to new pathways to explore in order to understand the neural substrates of BD pathophysiology and providing new cellular tools for novel therapeutic discovery.

METHODS

iPSC derivation and characterization

Fibroblast cell lines GM08330 (unaffected, father), GM08329 (unaffected, mother), GM05225 (BD Type I, proband), GM05224 (BD Type I, brother) were obtained from the Coriell Cell Repository. Records showed punch biopsies for GM05224 and GM05225 were collected from the posterior iliac crest as were the two parents GM08330 and GM08329 (Dr. Elliot Gershon, personal communication). Induced pluripotent stem cells (iPSCs) were derived using individual pseudotyped retroviruses expressing *MYC* (MSCV-h-c-MYC-IRES-GFP, Addgene# 18119), *KLF4* (pMIG-hKLF4, Addgene# 17227), *SOX2* (pMIG-hSOX2, Addgene# 17226), and *OCT4* (pMIG-hOCT4, Addgene#17225) packaged by Harvard Gene Therapy Core (Harvard Medical School) following methods described in[29]. Fibroblasts were infected with all four viruses as described[30] and split onto irradiated MEFs (GlobalStem, GSC-6301G). Colonies were picked and expanded in hES media on MEFs or in mTeSR1 on Matrigel. hES media consisted of 80% DMEM/F12 (Invitrogen, 11320033), 20% Knock-out Serum Replacement (KOSR) (Invitrogen, 10828-028), 10 ng/mL bFGF (R&D systems: Cat# 233-FB-001MG/CF), 1 mM L-glutamine (Invitrogen, 35050-061), 100 μM non-essential amino acids (Gibco, 11140-050), 100 μM 2-mercaptoethanol (Sigma, M6250), 50 U/mL penicillin 50 mg/mL streptomycin (Invitrogen, 15140-122), mTeSR1 (Stemcell Technologies, 05850).

Karyotyping

Cells were karyotyped by Cell Line Genetics (Madison, WI) with standard Giemsa stained chromosome spreads.

Teratoma formation

iPSCs were grown on Matrigel/mTesR1 media. For teratoma formation, ~10^7 iPSCs were pelleted and injected into SCID mice underneath the kidney capsule. Tumors were harvested after week 10 and analyzed using standard techniques with interpretation by Frank H. Lau (Cowan Lab, HMS, MGH).

Genetic analysis

Genomic DNA was isolated using the DNAEasy kit (Qiagen, 69504). Fingerprinting was carried out by the Broad Institute Genomics Platform using the Fluidigm platform according to the manufacturer's instructions. Whole-genome single nucleotide polymorphism (SNP) genotyping on 733,202 SNPs was carried out by the Broad Genomics Platform using Illumina OmniExpress arrays according to the manufacturer's instructions.

CNV analysis and validation

CNVs were detected using Birdsuite (version 1.6)[31]. Events with LOD score >/= 10 kb and size >/= 10kb were lifted onto HG19 using the UCSC browser's lift over tool. These spanned ~16 loci. One of these events (HG19:chr6:78973201-79029367) overlaps a region of common CNVs in HapMap[32]. CNVs were validated with either commercially available or custom designed TaqMan probes. Probes were - 6p22.1, HG19:chr6:29859709-29896421,

Hs03587795_cn (LifeTech), context sequence CAGGAGAATGTTCCTGCTGAGGACA; Chr9,HG19:chr9:7734481-7770942, Hs06879643_cn, context sequence AATAGCCTCATTACACCTTGCAAAT; 6q16.1, HG19:chr6:95486777-95578465, probe primer TCCATAATCAGCGTGGCATA, 5' 6-FAM ZEN 3'Iowa Black FQ, forward primer TCAGGGTTGGTTTGCTTATTG, reverse primer CACCAATATATGTTCAAAGGGTCA. Assays were carried out using digital droplet PCR (Bio-Rad) according to the manufacturer's instructions.

Identity-by-descent analysis

Using genotyping data generated by the Illumina Omni Express chip and PLINK[33], SNPs were pruned using pairwise genotypic correlation to identify informative markers and then IBD (Identity-by-Descent) proportions were calculated between all individuals. IBD estimates were compared with expected values to affirm relationships between the family members[34].

Multi-dimensional scaling analysis of SNP genotypes

For multi-dimensional analysis of SNP profiles, Family-811 quartet genotype data was merged with data from STEP and HapMap 2, and retained only those genotypes shared between all three datasets (N=180,564). Using PLINK[35], LD-based SNPs were pruned to 97,171 SNPs and then multi-dimensional scaling was run. Individuals from CEU (60) Western European, YRB (60) Yoruban, HCB (90) Han Chinese, STEP-BP (1753) and Family-811 (4) were analyzed.

Isolation of neural progenitor cells (NPCs)

NB/B27/EGF/FGF/Heparin medium (NPC induction media) was Neurobasal media (Invitrogen) supplemented with $1\times$ B27 (without retinoic acid) (Invitrogen,12587-010) $1\times$ penicillin/streptomycin (Invitrogen,15140-122), 2 mM L-glutamine (Invitrogen, 21051-024), 20 ng/mL EGF (Sigma-Aldrich, E9644), 20 ng/mL bFGF (R&D systems, 233-FB-001MG/CF), 5 μg/mL Heparin (Sigma, H3393). NPC maintenance media was knockout DMEM/F12 (Invitrogen, 15140-122), 2 mM GlutaMax-1 supplement (Invitrogen, 35050-061), $1\times$ Antibiotic-antimycotic (Invitrogen, 15240-062), 2% StemPro Neural supplement (Invitrogen, A10508-01), 5 μg/mL Heparin (Sigma, H3393), 20 ng/mL bFGF (R&D systems: Cat# 233-FB-001MG/CF), 20 ng/mL EGF (Sigma-Aldrich, E9644). Plate coating buffer was 15 μg/mL Poly-ornithine (Sigma, P4957), 10 μg/mL Laminin (Sigma, L2020). To initially isolate heterogeneous populations of NPCs, iPSC colonies were grown on MEFs in hES+bFGF medium. When confluent, colonies were treated with Dispase at 1 mg/mL and passaged to Matrigel (BD Biosciences, 354277) at approximately 10–20 iPSC colonies/well of a 6-well plate and cultured in hES+bFGF media. After 3 days, bFGF was withdrawn from the media and iPSCs were allowed to differentiate. Media was changed every 2 days. After 7 days, cultures were switched to NPC induction media and changed every other day until neural rosettes appeared. Neural rosettes were manually picked and transferred to poly-ornithine/laminin coated plates and cultured in NPC media. Cultures were fed every other day until confluent. Cells were passaged using TryplE at room temperature and plated at a density of 8×10^4 cells/cm^2.

Fluorescence activated cell sorting of neural progenitors

Conditions and fluorescence activated cell sorting (FACS) parameters were based on work of Yuan et al.[36]. Conjugated antibodies were purchased from BD Biosciences (San Diego): CD184-APC (clone 12G5), CD271-PerCPy5.5 (clone C40-1457), CD24-PE (clone ML5), CD15-FITC (clone HI98). FACS buffer consisted of 1× Hank's buffered solution, 2% fetal bovine serum, 20 mM glucose, 1× penicillin/streptomycin, 1 mM EDTA and was filtered and made fresh for each experiment. Accutase (Invitrogen, A11105-01), DNase I (Sigma, D4263), 1 unit /μL, DAPI (Invitrogen, D3571) was made at 2 mg/mL in H_2O. To obtain $CD184^+$, $CD271^-$, $CD24^+$, $CD15^+$ cells, mixed NPC populations were either immunoselected using EasySep CD184 (Stem Cell Technologies) according to the manufacturer's instructions and FACSed or directly FACSed. For preparing cells for FACS, $0.5–2×10^7$ cells were washed once with DMEM/F12 and dissociated with Accutase at 37°C for 5 minutes. FACS buffer was added to terminate digestion and cells were triturated to form a single cell suspension. Cells were then washed twice with FACS buffer and resuspended at a concentration of $1×10^7$ cells/mL. DNAse I was added to a final concentration of 100 units/mL and the suspension was incubated at room temperature for 10 minutes. Cells were stained immediately. $1×10^7$ cells/mL were stained for 20 minutes at 4°C with the respective single conjugated antibodies or all four conjugated antibodies with dilutions consisting of 1:12 CD184, 1:20 CD271, 1:12 CD24, and 1:12 CD15. Cells were washed once in FACS buffer and resuspended in 500 μL for single color staining and 1–2 mL for four color staining. Cells were maintained at 4°C until ready for sorting using a 4-color sorting protocol on a FACS Aria cell sorter to obtain $CD184^+$, $CD271^-$, $CD15^+$, $CD24^+$ cells (BD Biosciences). A gating protocol was established in which $CD184^+$ $CD271^-$ cells were separated into $CD24^+$ and $CD15^+$ containing populations. Cells were sorted directly into Neurobasal media at room temperature using a 100 μm nozzle, 20 psi sheath pressure, 2,000 events/sec; taking care not to subject the cells to excessive shear forces that would reduce viability. Cells were plated with ROCK Inhibitor (10 ng/mL) at a concentration of $1–4×10^5$ cells in one well of a six well plate or $0.5 – 0.9 ×10^5$ cells in one well of a 12-well plate.

Neuralized embryoid body formation

iPSCs were grown on MEFs or Matrigel to confluence. iPSCs were dissociated with Accutase (Invitrogen, A11105-01). 3,000–6,000 single cells were placed in Aggrewell 400 plates (Stemcell Technologies, 27945) and incubated in hES media without FGF for 24 hours. Aggregates were released and passed through the 40 μm cell strainer to remove single cells. 1,000 aggregates/well were plated in an ultra-low adherence 6-well plate (Corning, 3471) in Neural Induction medium on day 0. Neuralized embryoid bodies (nEBs) were fed every other day and harvested on days one and eleven for further analysis. RNA was isolated from EBs using the MicroRNAeasy kit (Qiagen, 217004).

Lineage scorecard analysis

iPSCs were cultured and dissociated as described for nEBs above. nEBs were formed in hES media without FGF for 16 days with media changes every two days. nEBs were harvested and RNA was collected using a MicroRNAeasy kit (Qiagen, 217004). Lineage scorecard

was calculated for nondirected EB differentiation using the NanoString probe set described by Bock et al. after quantification using single-molecule imaging on an nCounter System according to the manufacturer's instructions by the Meissner Lab at Harvard University.[37]

Neuronal differentiation

Cells were dissociated into a single cell suspension with TriplE (Invitrogen, 12604-013) or Accutase and 3×10^4 NPCs were plated on glass coverslips coated with 10 μg/mL laminin (Sigma, L2020) and 15 μg/mL poly-ornithine (Sigma, P4957) in Neurobasal media (Invitrogen, 21103-049) containing 200 μM ascorbic acid, 0.5 mM dibutyryl cAMP (Sigma, D0260), and 1 mg/mL laminin, 20 ng/mL BDNF (Preprotec, 450-02), 20ng/mL GDNF (Preprotec, 450-10). Cells were fed every two to three days until ready for immunostaining and/or electrophysiology.

Immunostaining

Cells were washed with PBS, fixed in 4% paraformaldehyde at room temperature for 15–20 minutes and permeablized with 100% ethanol for 2 minutes at room temperature. Fixed cells were blocked in 4% BSA, 0.1% Triton X-100, in PBS at room temperature for 1 hour. Primary antibodies diluted in 0.5% BSA, 0.1% Triton X-100 in PBS and incubated overnight at 4 °C. Following incubation cells were washed 3 times for 5 minutes each in PBS then incubated with secondary antibody Alexa-fluor 488-conjugated goat anti-mouse antibodies (1:500, Invitrogen A11017), Alexa-fluor 555-conjugated goat anti-rabbit (1:500, A21430), Alexa-fluor 647-conjugated goat anti-chicken antibodies (1:500, A21449) for 1 hour at room temperature. Cells were washed 3 times in PBS and subsequently mounted onto glass slides with prolong gold anti-fade reagent with DAPI (Invitrogen, P36931). Immunofluorescence was visualized with Nikon Eclipse 80i fluorescent microscope (Nikon, Japan). The following primary antibodies were used TuJ1 (anti-β-Tubulin III; 1:500, Sigma T2200), MAP2 (1:10000, Chemicon AB5622) and GFAP (1:200, Sigma G3893) (data not shown).

NanoString digital mRNA expression profiling

RNA was isolated using the miRNAEasy kit (Qiagen, 217004) according to the manufacturer's instructions. 100 ng of total RNA from each sample was profiled using single-molecule imaging on an nCounter System according to the manufacturer's instructions by the Genomics Platform at the Broad Institute using a 352 probe custom PsychGene probe set consisting of genes to profile pluripotency, differentiation, WNT signaling, and candidate genes previously associated with either BD or schizophrenia (Sup. Table 7). Data were normalized using spiked in positive and negative control genes and the VSN algorithm[38]. Differentially expressed genes were identified using the Bioconductor module limma[39].

RNA-seq transcriptome analysis

RNA was isolated using the miRNAEasy kit (Qiagen, 217004) according to the manufacturer's instructions. All libraries were molecularly barcoded using TruSeq adaptors (Illumina) and sequenced on a HiSeq2000 (Illumina) using paired-end 75 cycle reads. The

assembly of transcripts estimation of their abundances, and tests for differential expression were performed using Tophat (transcriptome version: Ensembl Homo_sapiens.GRCh37.73.gtf) and Cufflinks-Cuffdiff v1.0[40] (transcriptome version: Illumina's igenomes Ensembl GRCh37). To increase statistical power, FPKM values were averaged from both parental control CXCR4^{+} NPC samples and both replicates of the BD-patient CXCR4^{+} NPCs GM05224. Only transcripts with sufficient read depth in both conditions as determined by Cuffdiff analysis were considered in subsequent analysis.

BrdU incorporation assays of DNA replication

Cells were plated on poly-ornithine/laminin coated coverslips and grown for two days. BrdU (Sigma, B5002) was added to a final concentration of 10 μM for 2 hours at 37°C. Cells were fixed in 2% paraformaldehyde for 15 minutes at room temperature, and then permeablized in 95% methanol for 20 min at −20°C. DNA was denatured with 2 N HCl at room temperature for 10 minutes, neutralized in 0.1 M borate buffer (pH 8.5) for 10 minutes. Cells were blocked in 5% goat serum/0.2% Triton X-100/1% BSA/PBS at room temperature for 30–60 minutes. Cells were stained with mouse anti-BrdU (1:100, Sigma, B8434) and rabbit anti-NESTIN (1:2000, R&D Systems, MAB1259) antibodies. Cells were then stained with secondary antibodies goat anti-mouse Alexa 488 and goat anti-rabbit Alexa 555 (Molecular Probes Invitrogen, A21428). Coverslips were mounted with Vectashield and imaged. In 3 independent experiments, 300–500 cells were counted and percent BrdU incorporation was calculated as the total BrdU positive cells divided by the total NESTIN positive cells in a field. Statistical significance was calculated using ANOVA. CHIR-99021 effects on proliferation were measured in parallel cell cultures and were treated with DMSO (vehicle) and CHIR-99021 (custom synthesized as for Pan et al.[41]) at a final concentration of 5 μM for 16 hours before BrdU labeling.

Electrophysiology

Cells were differentiated as described above. Standard patch clamp recordings were carried out using an extracellular solution (in mM) consisting of 115 NaCl, 2 KCl, 3 CaCl$_2$, 10 glucose, 1.5 MgCl$_2$ and an intracellular (in mM) consisting of 140 potassium gluconate (C$_6$H$_{11}$KO$_7$), 5 KCl, 2 MgCl$_2$, 10 HEPES, 0.2 EGTA, 2.5 Na-ATP, 0.5 Na-GTP, 10 Na$_2$phosphocreatine. Voltage activated currents were recorded in the voltage clamp configuration using an Axopatch 200B patch clamp amplifier and head stage. Series resistance was compensated up to 80%. Action potentials were recorded in the current clamp configuration on the Axopatch 200B. Data was acquired using pClamp10 at a rate of 10 kHz filtering at 5 Hz. Data was analyzed using pClamp software and custom scripts written in Igor (Wavemetrics).

Network analysis, clustering and Gene Ontology analysis

Agglomerative hierarchical clustering with a weighted pair-group average was performed using a Pearson correlation coefficient as the similarity metric on the matrix of NanoString PsychGene probes that showed statistically significant differential expression in either the NPCs or neurons comparing the BD and unaffected parental control samples with XLSTAT (v2014.3.02). Disease Association Protein-Protein Link Evaluator (DAPPLE) v2.0 was run using the web based tool available at www.broadinstitute.org/mpg/dapple/dappleTMP.php.

The resulting direct and indirect network was constructed. Of the input seed list of 53 differentially expressed genes, 43 were mappable by DAPPLE while a subset of genes that were also differentially expressed (*C4ORF45, CACNG8, FNIP2, HLA-B, IRX3, NKX2.2, NKX6.1, POTED, SOX5, VEPH1*) were not. The p-value for the global network parameters and individual p-values for seed proteins representing the probability that by chance the seed protein would be as connected to other seed proteins (directly or indirectly) as is observed were calculated with 5,000 within-degree, node-label permutations. For Gene Ontology (GO) analysis of RNA-seq profiles, DAVIDv6.7 bioinformatics software was used to determine GO categories with significant representation (p<0.05, Benjamini-Hochberg corrected).

Results

We selected a subset of four individuals from a multigenerational kindred, Family-811 with bipolar disorder originally described by Gershon and colleague[42] (Fig. 1A). This subset, referred to here as the "Family-811 quartet", consisted of an unaffected father (GM08330) and mother (GM08329) and their two sons with BD (GM05225 and GM05224) (Fig. 1A; Sup. Table 1). Whole-genome SNP profiling of 733,202 markers was performed on fibroblast DNA. Analysis of these data using inheritance by descent measures confirmed the expected parent-child and sibling relationships of the Family-811 quartet (Fig. 1B; Sup. Table 2), and using multi-dimensional scaling analysis showed that the quartet clusters with the Northern and Western Europe (CEU) individuals from HapMap (Fig. 1C).

To annotate the genomes of Family-811 quartet with genetic variants of potential relevance to neuropsychiatric disorder etiology, we analyzed the whole-genome SNP profiles of the Family-811 quartet and confirmed the SNP genotypes of a subset of the peak risk variants from the most recent Psychiatric Genetics Consortium GWAS (Sup. Table 3). These targeted genotyping assays indicated that all four Family-811 members were homozygous reference for the BD risk allele in *SYNE1* and *ANK3*. GM08329 (mother) was heterozygous for the risk allele of *CACNA1C* while the remaining family members were homozygous reference for the BD risk allele. All family members in the quartet were heterozygous reference for the BD risk allele in *ODZ4* (*TNM4*) except GM05225 who was homozygous reference. Finally, all family members were found to be heterozygous reference for a *ZNF804A* schizophrenia risk allele.

Using the whole-genome SNP data, with a criteria of LOD score > 10 and a size > 10 kilobases[31], several copy number variants (CNVs) were identified that segregated from parent to offspring (Fig. 1D, E; Sup. Table 4 & 5; Sup. Fig. 1). One CNV greater than 100 kb was identified in cytoband 9p24.1, near, but not identical, to a region previously identified in scans of psychiatric disorder patients by Malhotra et al.[43]. Three of the CNVs (6q16.1, 6q22.1, and 9p24.1) were subsequently validated in DNA isolated from lymphoblastoid cell lines from the Familly-811 quartet. Overall, these genomic data are consistent with the ethnicity of previous descriptions of members of Family-811, and it revealed that the BD patients contained no detectable large (> 10 kb) *de novo* structural genomic variants unique to both BD patients suggesting that CNVs of this nature are

unlikely to influence any observed cellular phenotypes unless introduced spontaneously during reprograming.

iPSC generation, characterization, and neural differentiation from Family-811

Using classical Yamanaka factors[15] (*OCT4, SOX2, KLF4 and cMYC*) delivered in retroviral vectors, at least three iPSC colonies from each fibroblast line from all four Family-811 quartet members were isolated, expanded, and fully characterized. All 12 iPSC lines were picked from primary iPSC colonies prior to any splitting and were expanded separately and thus can be considered independent iPSCs lines. Karyotype analysis indicated all 12 iPSCs were normal (Sup. Fig. 2), and a 23 SNP marker panel used for fingerprinting iPSCs post-reprogramming corresponded to their respective parental fibroblast lines (data not shown). Pluripotency of all 12 iPSC lines from the quartet was initially assessed through measurement of a panel of characteristic pluripotency markers, including NANOG, OCT4, SSEA-4, Tra-1-60 and Tra-1-81 (Sup. Fig. 3). As a further test of pluripotency, genome-wide transcriptome profiles were generated from all 12 iPSCs and PluriTest, a bioinformatic assay that uses global gene expression profiles to bench mark unknown iPSCs with *bona fide* pluripotent cells[44], was performed. The results of the PluriTest confirmed that the 12 iPSCs were highly similar in their transcriptome to previously described pluripotent stem cells (Sup. Fig. 4). Finally, pluripotency was directly assessed by determining the ability of all 12 iPSCs lines to form teratomas in nude mice. Upon sectioning and H&E staining, teratomas from all 12 iPSCs were found to contain representative tissue of all three (ectoderm, mesoderm, endoderm) germ layers (Sup. Fig. 5). Collectively, these data demonstrate successful generation of 12 high-quality, independent iPSC lines (picked from unique primary iPSC clones) from a family with BD.

To more specifically investigate the *in vitro* neural differentiation capacity of each of the 12 iPSCs lines from the Family-811 quartet, directed neural differentiation was used to generate NPCs. To initially derive heterogeneous populations of NPCs containing both central nervous system (CNS) and peripheral nervous system (PNS) progenitors, each of the 12 iPSC lines were cultured individually on MEF feeder cells and colonies were passaged manually to feeder-free cultures on Matrigel in the presence of bFGF. After 3 days, bFGF was withdrawn to induce differentiation and after 7 days the media was switched to neural induction media consisting of Neurobasal media supplemented with B27 (without retinoic acid), EGF and bFGF. All 12 of the iPSC lines, regardless of whether they were from the healthy control parents or BD sons, were found to be capable of forming neural rosettes with a morphology characteristic of early neuroepithelium, which upon picking and expansion on poly-ornithine/laminin coated plates gave rise to self-renewing NPCs that stained for a panel of markers, including SOX1, SOX2, NESTIN and MUSASHI (Fig. 2A and data not shown).

Next, to create more homogenous populations of NPCs that were enriched for CNS progenitors the initially mixed NPC cultures were immunopurified using a four color, fluorescence activated cell sorting (FACS) protocol designed to remove non-neural cells and cells expressing CD271 (p75; NGFR), a marker of neural crest cells that produce PNS cells and select for CD184 (CXC chemokine receptor-4 (CXCR4)) expression as a marker of CNS progenitors. (Fig. 2B, Sup. Fig. 6)[36]. Whereas self-renewing, CD184^{+}/CD271^{−}/

CD24$^+$/CD15$^+$ cells capable of expansion for more than five passages could be readily established from both the mother and father, neural induction of iPSCs from both BD patients repeatedly produced more PNS progenitors than CNS progenitors as defined by immunostaining for CD271 and CD184 markers, respectively (Sup. Fig. 7). Consistent with this phenotype, despite repeated attempts under varied neural induction conditions, CD184$^+$/CD271$^−$/CD24$^+$/CD15$^+$ immunopurified NPC lines could only be successfully established beyond five passages from a subset of the BD-patient iPSC lines. Of the successfully FACS-purified NPC lines expressing CD184$^+$, all had characteristic NESTIN$^+$ cell morphology, proliferated in a monolayer in the presence of EGF and bFGF, and upon mitogen removal differentiated into MAP2$^+$ and βIII-tubulin$^+$ (Tuj1$^+$) neurons capable of firing action potentials (Fig. 2B, C; Sup. Fig. 8). Thus, as summarized in the lineage diagram shown in Figure 2D, we were able to generate expandable (greater than five passages), FACS-immunopurified, CXCR4$^+$ NPC lines from all six of the parental iPSC lines and only one of three iPSC lines from each BD-affected son within the Family-811 quartet.

The successful generation of expandable CXCR4$^+$ NPCs lines from the parental control iPSCs and one iPSC from each of the BD-affected sons within the Family-811 quartet afforded the opportunity, for the first time, to characterize the molecular and cellular phenotypes in a defined CNS progenitor cell (i.e. CXCR4$^+$) and post-mitotic neurons derived from them upon neural differentiation. Initially, using bromo-deoxyuridine (BrdU) incorporation into DNA to measure cell proliferation, we observed a proliferation deficit in both of the BD patient NPCs compared to the unaffected parental NPCs (Fig. 3A, B) (t-test, p=0.001). In addition to this proliferation defect, both BD-patient NPCs produced qualitatively fewer βIII-tubulin (Tuj1$^+$) neurons than the unaffected NPCs over a six week differentiation time course (Fig. 3C). Taken together, these observations, and the difficulty encountered in generating CXCR4$^+$ NPCs from neural rosettes by FACS, collectively provided initial evidence for a neural differentiation deficit phenotype in both BD-patient NPCs from the Family-811 quartet that ultimately negatively impacts *ex vivo* neurogenesis.

NanoString molecular profiling of iPSCs, NPCs and neurons from Family-811

Having observed a neurogenesis deficit from the BD-patient iPSCs, to ensure that that the differentiation deficit did not represent a general differentiation defect of the iPSCs, we turned to an evaluation of the overall differentiation capacity of all 12 of iPSCs from the Family-811 quartet that we had generated. For these measurements, three independent iPSCs lines from each of the unaffected parents (6 lines total) and three independent iPSCs lines from the BD sons were grown (6 lines total) for 16 days under non-directed differentiation conditions and total RNA was isolated. The expression of a panel of 500 genes designed by Bock and colleagues as a "scorecard" to quantitatively define the differentiation capacity of human embryonic stem cell (ESCs)/iPSCs of unknown developmental capacity was then assessed using NanoString digital mRNA expression profiling technology, a highly sensitive, single-molecule imaging of color-coded, molecular barcoded probes (Sup. Table 6)[37]. Using this scorecard, we found no correlation between an iPSC line's ability to establish NPCs and its predicted differentiation capacity into ectoderm-derived cell types or the expression of a broad set of endodermal and mesodermal markers (Sup. Fig. 9, 10). Taken together with the pluripotency marker analysis, teratoma formation assays and

PluriTest assay results, these findings on all 12 of the iPSCs indicate that the BD-patient iPSCs do not exhibit a general differentiation defect that could otherwise confound the interpretation of the deficits in neural differentiation that we observed.

Having established the capacity of all 12 of the Family-811 quartet iPSCs to differentiate into multiple cell lineages, we next sought to further establish the nature of the neurodevelopmental deficits that were observed. For this, we again isolated total RNA from replicate cultures of fibroblasts, iPSCs, CXCR4+ NPCs, and six week differentiated neurons from the Family-811 quartet and used NanoString digital mRNA profiling to generate molecular signatures of each cell line using a custom "PsychGene" probe set rather than the Bock scorecard. This PsychGene probe set was specifically designed to measure the expression of 352 genes and consisted of pluripotency genes, neural patterning genes, WNT pathway genes and genes implicated in the genetics of neuropsychiatric disorders (Sup. Table 7)[12,45]. Using principle component analysis (PCA) to analyze the global PsychGene mRNA signature, we found that the respective cell types clustered together (Fig. 4A). Consistent with the results of this global analysis and our previous characterization of the iPSC properties, analysis of the expression of pluripotency and neural stem cell markers in all 12 iPSC lines confirmed the expected changes in expression of these genes when comparing the various cell differentiation states (Fig. 4B).

To better delineate the phenotypic defects in the BD patient cell lines from the Family-811 quartet, we then examined the average differences in gene expression of the BD patient cells relative to the unaffected parental control cells using the PsychGene NanoString probe set. Starting with the fibroblasts, examination of volcano plots in which the Log_2(fold change) was plotted against the $-\text{Log}_{10}$(p-value) revealed that only one gene, *ZIC1* (ZIC family member 1), a C2H2-type zinc finger transcription factor, met the criteria for a significant expression difference (fold change = 13.3, p-value = 0.04, Benjamini-Hochberg corrected) (Fig. 4C). For iPSCs, there were no genes that exhibited a significant difference in expression between the six control lines and 6 BD patient lines. In sharp contrast to the lack of multiple differentially expressed genes in the fibroblasts and iPSC cell states, when comparing the expression profiles of the FACS-purified NPCs there were 18 genes with significant expression differences between BD-patient NPCs relative to unaffected parental control NPCs (> 1.5 fold change; p-value < 0.05, Benjamini-Hochberg corrected) (Fig. 4C; Fig. 5A). Amongst this set of differentially expression genes in the BD-patient NPCs were three genes encoding homeodomain-containing transcription factors, *NKX2-2* (NK2 homeobox 2), *NKX6-1* (NK6 homeobox 1), *and IRX3* (iroquois homeobox 3) that are known to function in Sonic Hedgehog (SHH)-dependent neural patterning to specify the identity of ventral progenitor-derived neurons. In addition several NPC specific genes were differentially downregulated in the BD-patient NPCs: *PAX6* (paired box gene 6a), *DACH1* (dachshund homolog 1), and *PLZF* (promyelocytic leukemia zinc finger protein; *ZBTB16*), along with *DISC1* (disrupted in schizophrenia 1), the latter of which has been shown to be critical for the regulation of neurogenesis and is implicated in the etiology of multiple neuropsychiatric disorders[9,11,46,47].

To build on the differential gene expression signatures observed in the NPC state, we next analyzed the PsychGene NanoString profiles in post-mitotic, neurons that were

differentiated for six weeks. As expected, there was an increased expression of the general neural differentiation markers *DCX* (Doublecortin) and *MAP2* (Microtubule-associated protein 2), as well as expression of multiple markers of upper and lower layer cortical projection neurons, including *SATB*2 (Special AT-rich sequence binding protein 2), *CTIP2* (COUP TF-interacting protein 2; BCL11B), *ETV1* (Ets variant gene 1), *CUX1* (Cut-like homeobox 1), and *RELN* (Reelin) (Sup. Fig. 11). Comparison of the expression levels in BD-patient neurons relative to their unaffected parental controls revealed that 28 genes in the PsychGene profiles were upregulated (> 1.5 fold change and p-value < 0.05, Benjamini-Hochberg corrected), while 16 genes were down regulated (> 1.5 fold change and p-value < 0.05, Benjamini-Hochberg corrected) (Fig. 4C; Fig. 5B). Given the desire to gain insight into specific neuronal subtypes that may underlie alterations in the neurocircuitry affected in BD, analysis of the expression of markers of specific neuron subtypes revealed differential expression of only the cortical layer maker *CTIP2 (BCL11B)* and *RELN*, which were both significantly downregulated in the BD-patient neurons compared to neurons from the unaffected parents (Fig. 4C; 5B), while numerous other markers of defined neuronal subtypes showed no difference (Sup. Fig. 11). In this context, *CTIP2* is notable as it is a component of the nucleosome remodeling and deacetylation (NuRD) complex[48], which plays a key role in the epigenetic regulation of neurogenesis[49] and the differentiation of cortical layer V/VI subcerebral projection neurons[50]. *RELN*, an extracellular matrix glycoprotein, in contrast, is involved in cortical neuron migration[51]. Taken together, these results provide further support for our hypothesis that differentiation into specific neural lineages is disrupted in the BD-patient iPSCs when comparing FACS-purified CXCR4^{+} NPCs.

Having confirmed successful neural differentiation and observed differential gene expression amongst the BD-patient CXCR4^{+} NPCs and neurons relative to unaffected parental controls, we sought to link these gene expression differences directly to known genetic risk factors neuropsychiatric disorders. To do so, we first analyzed if several genes implicated by recent GWAS by the Psychiatric GWAS Consortium[52–54], *ANK3* (Ankyrin 3), *CACNA1C* (Calcium channel, voltage-dependent, L type, alpha 1C subunit), *ODZ4* (Odd Oz/ten-m homolog 4) and *ZNF804A* (Zinc finger protein 804A), were differentially expressed in the Family-811 quartet cells. While all four of these genes were expressed and exhibited increased expression after six weeks of neural differentiation, none were found to be differentially expressed between the BD patient and unaffected parent cells (Sup. Fig. 12).

Since we noted that a number of the genes were differentially expressed in both BD patients CXCR4^{+} NPCs and their differentiated neuronal progeny, in order to obtain a global view of the patterns of gene expression we used agglomerative hierarchical clustering to analyze a binary matrix of the total set of 53 significantly dysregulated genes. As shown in Figure 5C, a total of eight categories of genes were identified, including those such as *SYN1, SCN2A, CNTN6,* and *NKX2.2* that were upregulated in both cell states, as well as genes with opposite patterns of expression, such as *PAX6, DCX, PLZF* that were downregulated in NPCs, but upregulated in neurons. Given that the latter three genes are all considered markers of neural

progenitors, these data support the notion of the altered neurodevelopment upon directed differentiation of BD iPSCs.

Besides differential expression of neurodevelopmental genes, when analyzing the function of the other genes in the PsychGene NanoString profiles that showed significant expression differences, we noted, that, consistent with prior genetic studies implicating calcium channel genes[55,56], five of the 34 (~15%) differentially expressed genes in the BD-patient neurons were calcium channel or other ion channel subunits (Fig. 5B): *CACNA1E* (calcium channel, voltage-dependent, R type, alpha 1E subunit; Cav2.3), *CACNA1G* (calcium channel, voltage-dependent, T type, alpha 1G subunit; Cav3.1), *CACNB1* (calcium channel voltage-dependent beta 1 subunit), a regulator of alpha-1 subunit membrane targeting and voltage dependent activation and inactivation, *CACNG8* (calcium channel, voltage-dependent, gamma subunit 8), a regulator of AMPA (α-amino-3-hydroxy-5-methyl-4-isoxazolepropionic acid) receptor localization, the sodium channel genes *SCN2A* (sodium channel, voltage -gated, type II, alpha subunit; Nav1.2) and *SCN3A* (sodium channel, voltage -gated, type III, alpha subunit; Nav1.3). However, due to the fact that our NanoString PsychGene probe set was purposely biased in its construction for coverage of genes relevant to neurodevelopment and neuropsychiatric disorder, it was not possible to calculate whether there was significant enrichment of any given functional category of genes amongst the set of differentially expressed genes.

As an alternative approach to determining if there was evidence for common underlying molecular pathways, we turned to the consideration of the protein-protein interaction network amongst the proteins encodes by the differentially expressed genes. Using Disease Association Protein-Protein Link Evaluator (DAPPLE) v2.0, the set of the 53 differentially regulated genes were used as seed nodes and we built a direct and indirect (through other proteins) interaction network amongst the proteins encoded by the seed genes with edges between the nodes derived from protein-protein interaction data in the InWeb database of protein interaction that combines multiple data sources (MINT, BIND, IntAct, KEGG, ECrel, Reactome) as described by Lage et al.[57] (Sup. Fig. 13A). The statistical significance of the connectivity of individual proteins to other seed proteins, as well as a set of network connectivity parameters, was then assessed with within-degree, node-label permutation methods. Of the input 43 seed genes that could be mapped, 9 proteins (MAP2, GPM6A, CACNA1G, CACNA1E, KLF4, CDH2, DACH1, SCN3A, SOX2) showed statistically significant (p<0.05) connectivity after a 5,000 within-degree, node-label permutation (Sup. Tables 8 & 9). Amongst the direct interactions between seed genes (Sup. Fig. 13B), there were 5 protein pairs consisting of: i) PAX6--SOX2; ii) CTIP2--NR2F1; iii) MAPT--NEFM; iv) MAP2--CDH2; and v) SCN2A--SNC3A, which was more than expected by chance alone (p=0.04, 5,000 permutations). In terms of the global network connectivity parameters, the network was composed of a total of 433 interactions from 220 unique proteins. Whereas the mean associated protein direct connectivity was not significant, the observed mean associated protein indirect connectivity (16.7; p=0.0058, 5,000 permutations) was nearly twice that expected. Taken together, these data support the hypothesis that there are shared functional pathways that are differentially regulated in the BD patients CXCR4+ NPCs and neurons compared to their parental controls. Furthermore, the network analysis points to

specific physical protein-protein interaction networks that may be key mediators of the underlying phenotypic differences, including the transcription factors PAX6 and SOX2, the chromatin regulator CTIP2 and its direct interactor NR2F1 (Nuclear Receptor subfamily 2, group F, member 1), a member of the nuclear hormone receptor family of receptors, and the calcium channel subunits CACNA1G and CACNA1E.

Global transcriptome analysis of BD patient NPCs versus their parental controls

In order to validate the differential expression of genes in the BD patient-derived cells that was observed in the PsychGene NanoString profiles, and in order to specifically characterize the BD patient-derived cells in greater depth, we performed genome-wide, transcriptome analysis using RNA-sequencing (RNA-seq) to compare the BD patient CXCR4^{+} NPCs and parental control CXCR4^{+} NPCs since this was the cell state that showed the earliest evidence of multiple robust phenotypic differences in the NanoString analysis. Total RNA was collected from each of the parental CXCR4^{+} NPC lines and replicate cultures of one of the BD patient CXCR4^{+} NPCs. Tophat was used to align raw RNA-seq reads to the Ensembl human transcriptome followed by Cuffdiff v1.0 identification of differentially expressed genes from averaged reads from both parents and averaged reads from both replicates of the BD CXCR4^{+} NPCs. In total, 15,803 transcripts, including both coding and non-coding transcripts were measured with sufficient coverage in both samples, of which 503 were found to have nominally significant differential expression ($p<0.05$), which after correction for multiple hypothesis a total of 35 were considered significantly expressed ($p<0.05$, Benjamini-Hochberg) (Sup. Table 10).

Having these orthogonally generated mRNA quantification data we sought to first cross-validate these data with our differentially expressed genes observed from the PsychGene NanoString molecular profiles of the CXCR4^{+} NPCs. As summarized in Supplementary Figure 14, of the 15 genes analyzable by both methods, we observed concordant results for four (80%) of the five upregulated transcripts and six (60%) of the downregulated transcripts. Given the vastly different nature of the assays, with discrepancies being possible due to differences in transcripts considers and sensitivity of the methods, these results overall provide confidence in the reproducibility of the molecular profiles.

Next, to determine whether the set of 503 transcripts covered any significantly overrepresented Gene Ontology (GO) terms suggestive of common process and pathways, we analyzed the set using DAVIDv6.7 bioinformatics software (Table 1; Sup. Table 11). Of the 412 transcripts that could be mapped, 18 GO terms associated with the category of Biological Process were found to be significantly overrepresented ($>3\times$; $p<0.05$, Benjamini-Hochberg) with the most enriched being those concerning *Neuron Differentiation, Development*, and *Morphogenesis*. At the same level of enrichment and significance, a total of six Cellular Compartment terms were overrepresented, including multiple terms covering the extracellular matrix and chromatin. Taken together, these data are overall supportive of our conclusions from the molecular profiling using the PsychGene NanoString probe set that are differences in expression of genes important for neurodevelopment and neurogenesis in the BD patient CXCR4^{+} NPCs compared to their unaffected parental controls.

Using the set of 503 nominally significantly, differentially expressed transcripts as input seeds, we again constructed a protein-protein interaction network using DAPPLE v2.0 (Sup. Fig. 15). Of the input 256 seed genes that could be mapped, 23 proteins showed statistically significant (p<0.05) connectivity after a 5,000 within-degree, node-label permutation (Sup. Table 12). Amongst the direct interactions between seed genes, there were 113, which was more than expected by chance alone as evaluated by permutation testing (p=0.0008). In terms of the global network connectivity parameters, the network was composed of a total of 5,471 interactions between 1,719 unique proteins, with both the observed mean associated protein direct connectivity (1.9; p=0.045) and the observed mean associated protein indirect connectivity (89.5; p=0.0002) significant with 5,000 permutations (Sup. Fig. 15). Taken together with the GO category analysis and similar analysis from using the PsychGene NanoString profiles, these data strongly support the hypothesis that there are shared functional pathways that are differentially regulated in the BD patients CXCR4^{+} NPCs compared to their parental controls.

Rescue of proliferation defects in BD-patient NPCs with GSK3 inhibition

One gene identified as down regulated in the BD patient CXCR4^{+} NPCs in the RNA-seq profiles that was found to be significantly highly connected (p<0.005; 5,000 permutations) within the DAPPLE network was that of Wingless-Type MMTV integration site family, member 7B (WNT7B), which had direct interactions with four other seed nodes consisting of two members of the frizzled family of seven transmembrane receptors (FZD5, FZD7) and two soluble frizzled-related proteins (SFRP1, SFRP2) (Fig. 5E). Collectively, the proteins within this module are known to play key roles in the regulation of WNT signaling, which is known as critical mediator of neurogenesis, neurodevelopment, and synaptic plasticity. Motivated by these observations, the previously observed differential expression of multiple WNT pathway components in both the PsychGene NanoString profiles (Fig. 5A, B), along with previous implication of WNT/GSK3 signaling in BD in part through the ability of lithium to activate WNT signaling[12–14], we hypothesized that activation of WNT signaling through GSK3 inhibition would be sufficient to rescue the NPC proliferation deficits observed in the FACS-purified, BD patient-derived CXCR4^{+}. In agreement with this notion, as shown in Figure 5F and Supplemental Figure 16, treatment with CHIR-99021 (5 μM; 16 hr), a highly selective and potent GSK3 inhibitor[41,58], led to a significant increase in BrdU incorporation in both BD-patient NPC lines. In parallel, we assessed the response of the NPCs to CHIR-99021 treatment at the level of expression of known WNT pathway genes using our PsychGene NanoString probe set. As summarized in (Fig. 5G), CHIR-99021 treatment (5 μM; 16 hr) increased the expression of the β-catenin target genes *LEF1* (Lymphoid enhancer-binding factor 1) and *AXIN2* (Axis inhibition protein 2), both of which are critical regulators of canonical WNT signaling. Taken together, these results suggest that WNT pathway activation can rescue the neurogenesis defects observed in the BD-patient CXCR4^{+} NPCs from the Family-811 quartet.

Gene expression analysis of neutralized embryoid bodies from Family-811 iPSCs

To further corroborate our findings of differential gene expression between the BD patient CXCR4^{+} NPCs and neurons compared to their parental controls, and to overcome the limitation of having only one expandable CXCR4^{+} NPC line from each of the BD patient

iPSCs, as an alternative differentiation method we turned to the generation of neutralized embryoid bodies (nEBs) formed from aggregating iPSCs under conditions that promote neuroectoderm formation (Sup. Fig. 17–19). Whole cell RNA was collected from multiple BD and unaffected nEBs at day one and day eleven. Using qRT-PCR, as expected, neuralization resulted in increased expression of *SOX1* (SRY-box containing gene 1), a transcription factor that is an early maker of neuroectoderm formation, in both the unaffected and BD-patient iPSC lines. In contrast, two of the BD-patient nEBs failed to express *PAX6*, an evolutionarily conserved, homeobox-containing transcription factor downstream of *SOX1* that plays an essential role in balancing cortical neural progenitor proliferation and differentiation[59,60], whereas both unaffected parental lines upregulated *PAX6* expression (Supp. Fig. 17). This downregulation of *PAX6* expression in the BD-patient nEBs was in agreement with the reduced *PAX6* expression observed by the NanoString profiles in the FACS-isolated CXCR4+ NPCs and by RNA-seq (Fig. 5A; Sup. Fig. 14). Taken together, these data suggest the dysregulation of *PAX6* expression, a key regulator of corticogenesis, contributes to the neural differentiation deficit of the BD patient iPSCs from Family-811.

Upon observing aberrant expression of the NPC marker *PAX6* in the BD patient nEBs, we next tested an expanded set of 48 genes consisting of differentially expressed genes identified from our PsychGene NanoString assays of the FACS-purified CXCR4+ NPCs along with WNT, NOTCH, and SHH pathway genes using the Fluidigm BioMark HD system (Sup. Fig. 18 & 19; Sup. Table 13). As expected, pluripotency genes, *SOX2, OCT4* and *NANOG* were repressed upon nEB formation to similar extents comparing the BD and unaffected parental iPSCs. Significant differential expression of *NKX6-1, LEF1, NEUROG1, NRG3*, and *SPARCL1* in the BD nEBs relative to the unaffected parental controls was observed (Sup Fig. 18 & 19). Taken together with the results from the analysis of the CXCR4+ NPCs using NanoString and RNA-seq, these finding provide further evidence for differential gene expression upon induction of neurodevelopment in the BD patient-derived cells compared to their parental controls from Family-811.

Discussion

A number of issues inherent to modeling complex, polygenic diseases with patient-derived stem cells complicate the unambiguous association of *in vitro* phenotypes with disease pathogenesis. Most notably, given the complex genetic architecture, potential genetic diversity of each individual cell line, and also the technical variability in the isolation of iPSC lines, the studies performed to date, including those described here, have all been underpowered to rigorously test hypotheses about disease etiology and the relationship of specific genetic variants to cellular phenotypes.

In this work, we sought to simplify the question of genetic diversity by using genetically related individuals rather than genetically unrelated cases and controls under what we consider a family-based paradigm for iPSC modeling of complex human genetic disorder. To this end, we generated clonally independent iPSCs (rather than clones derived from the same founding cell line), as well as highly purified, expandable, CXCR4+ NPCs from multiple members of the same family with unaffected and BD individuals. This family-

based paradigm using a pedigree enriched for neuropsychiatric phenotypes[42], has the advantage of controlling for genetic background, and enhancing the chance that both affected individuals share the same underlying BD etiology. In the future, as higher throughput methods for iPSC generation are brought to bear, following such a paradigm will allow the field to carry out more adequately powered studies. Given the density of psychopathology found within the pedigree of Family-811 from which the nuclear family we reprogrammed was derived, a priority for the future should be to reprogram additional family members for which fibroblasts already exist in order determine whether other family members with BD exhibit the same phenotypes relative to other unaffected family members.

Overall, our phenotypic characterization of the two affected BD sons to their unaffected parents at the level of cellular and molecule profiles revealed a number of significant and consistent differences (summarized in Sup. Table 14). Given the neurodevelopmental phenotypes we observed in the BD iPSCs relative to their parental controls, of paramount importance to the interpretation of these results was to demonstrate that the BD iPSCs did not exhibit generic differences in their pluripotency and capacity to differentiate into other non-neuronal tissues. We addressed this potential concern for all 12 iPSCs lines three ways: 1) demonstrating the expression of a panel of appropriate pluripotency markers through immunostaining and mRNA assays; 2) demonstrating the capacity to form multiple germ layers through *in vivo* teratoma formation; and 3) genome-wide expression profiling and the use of PluriTest as a computational method to benchmark our iPSCs to other pluripotent stem cells. After first establishing the pluripotency of all three iPSCs generated from each of the Family-811 quartet members through multiple methods, and demonstrating a lack of an overall differentiation deficit into multiple germ layers, our results point to specific defects in this family in the development, establishment or maintenance of NPCs, potentially due to the dysregulation of *PAX6*, an essential regulator of neurogenesis and corticogenesis.

Although the generalizability of these observations will require the creation of iPSCs from additional BD patients, which is ongoing, two other studies in the context of psychiatric disorders that described the isolation of similar NPCs did not describe phenotypic defects in these types of cells[25,61]. While this manuscript was under revision, a study by Chen et al.[62] described a set of BD patient-derived iPSCs. While Chen et al. did not characterize phenotypes of BD NPCs, when differentiated neuronal cells derived from neuronal rosettes were examined, encouragingly several gene expression changes that overlap with those identified in our iPSC-derived cells from Family-811 were observed. First, *PAX6* gene expression was altered in both studies: Chen et al. showed *PAX6* expression was decreased in BD patient neurons; our data suggest *PAX6* expression is decreased in BD patient NPCs, but in our studies *PAX6* expression in the culture was increased upon further differentiation into neurons (Fig. 5A, B). While the direction of the *PAX6* effect in neurons is different, both of these BD iPSC studies are consistent with there being an alteration in the normal fate of neuronal differentiation in BD iPSCs. These differences may arise from the use of a different neuron/NPC differentiation protocol as in Chen et al., control and BD neurons were derived from iPSC aggregates in which neural induction was performed using dual SMAD inhibition with subsequent manual passaging and expansion of rosettes followed by differentiation into neurons; our NPC derivations begin in a monolayer and did not use dual

SMAD inhibition. Alternatively, these differences may be inherent to the particular BD patients investigated. Similar to our results, Chen et al. also identified changes in the calcium channel subunit *CACNA1E*, although once again the direction of the change was different. Our data also suggest other calcium channel subunits are altered *(e.g. CACNA1E, CACNA1G, CACNB1, CACNG8* (Fig. 5B)), consistent with calcium signaling being altered in neurons from BD patients. Another similarity in the gene expression data were *FGF14* levels: both studies show *FGF14* levels are increased in BD neurons. FGF14 is a nonsecreted FGF that associates with sodium channel complexes[63–66] and regulates their function along with the function of presynaptic calcium channels[67]. Furthermore, FGF14 localizes at the axonal initial segment (AIS) where Ankyrin G (encoded by *ANK3*), a BD risk gene, clusters sodium channels[64,68]. Lastly these FGF14/sodium channel complexes have been shown to be regulated by GSK3[69], a target of the BD therapeutic lithium and the inhibitor CHIR-99021 used in our study to rescue the proliferation deficit seen in BD patient NPCs. While these gene expression data suggest a functional connection between FGF14 and other BD risk associated genes, there has been to date no significant genetic association between *FGF14* and bipolar disorder risk in the Psychiatric GWAS consortium's analysis[70]. Nevertheless, taken together, these consistent gene expression changes and functional themes suggest that there may be several connections between genes altered in iPSC-derived BD neurons and other risk associated genes and pathways that implicate calcium signaling and AIS function as nodes of integration of BD pathogenesis.

Besides the cellular-level phenotypic differences in NPC formation and neurogenesis, at the molecular level several groups of differentially expressed genes were observed further supporting the notion of neurodevelopmental abnormalities in the BD-patient NPCs and neurons. Of note, *CNTN6* (Contactin-6; NB-3), a cell adhesion molecule also implicated in autism[71], which has shown modest association (rs3772277; p = 0.000126) with BD in the Psychiatric GWAS Consortium study[70], and was significantly associated with a BD subgroup with co-morbidities in the GAIN cohort[72] (rs2727943; p = 3.3×10^{-8}) was among the most differentially expressed genes in both the NanoString and RNA-seq profiling (Fig. 4C; 5A, B). Previous work suggests that Contactin-6 plays a role in maturation of oligodendrocyte progenitors through its interaction with Notch1, a key regulator of neurogenesis[73], potentially pointing to perturbation of oligodendrocyte development in the BD-patient iPSCs. Future studies aimed in investigating whether there are oligodendrocyte abnormalities in these and other BD iPSC models is warranted. Finally, several results from our studies suggest WNT signaling is perturbed in the neural cells from the two BD affected sons. First, in both our NPCs and nEBs, we identified multiple genes involved in WNT signaling that were differentially expressed between the BD and parental lines. Second, rescue of the proliferation defect in the BD-patient NPCs from Family-811 upon treatment with CHIR-99021, a highly potent, and selective GSK3 inhibitor[41], suggest dysregulation of the WNT pathway may underlie at least a subset of the phenotypic differences observed in the BD-patient NPCs. Given the ability of the BD therapeutic lithium to activate WNT signaling, these findings support the notion that targeting the WNT/GSK3 pathway may provide an important direction for the development of novel therapeutics for BD[74].

In summary, with the generation of this set of 12 iPSCs along with a set of representative expandable NPC lines for the first time from a family with BD, our studies have established a new paradigm and resource for gaining insight into the etiology and pathogenesis of BD. Collectively, our phenotypic comparisons present numerous avenues for future investigation through the implication of abnormalities in early steps in NPC formation, WNT/GSK3 signaling, and ion channels expression in the BD patient-derived NPCs and neurons. Future expansion of these studies to include samples from additional families and well phenotyped patients along with appropriately selected controls holds tremendous promise for helping elucidate fundamental mechanisms of human disease biology and for presenting a new path for translating basic research into novel therapeutic discoveries for BD[74].

Supplementary Material

Refer to Web version on PubMed Central for supplementary material.

ACKNOWLEGEMENTS

REFERENCES

1. Newberg AR, Catapano LA, Zarate CA, Manji HK. Neurobiology of bipolar disorder. Expert Rev Neurother. 2008; 8:93–110. [PubMed: 18088203]

2. Cataldo AM, et al. Abnormalities in mitochondrial structure in cells from patients with bipolar disorder. Am J Pathol. 2010; 177:575–585. [PubMed: 20566748]

3. Soeiro-de-Souza MG, et al. Translating neurotrophic and cellular plasticity: from pathophysiology to improved therapeutics for bipolar disorder. Acta Psychiatr Scand. 2012; 126:332–341. [PubMed: 22676371]

4. Mendlewicz J, Rainer JD. Adoption study supporting genetic transmission in manic--depressive illness. Nature. 1977; 268:327–329. [PubMed: 887159]

5. Craddock N, Sklar P. Genetics of bipolar disorder. Lancet. 2013; 381:1654–1662. [PubMed: 23663951]

6. Purcell SM, et al. Common polygenic variation contributes to risk of schizophrenia and bipolar disorder. Nature. 2009; 460:748–752. [PubMed: 19571811]

7. Group., P. G. C. B. D. W. Genome-wide association study identifies five new schizophrenia loci. Nature genetics. 2011; 43:969–976. [PubMed: 21926974]

8. Phillips ML, Swartz HA. A critical appraisal of neuroimaging studies of bipolar disorder: toward a new conceptualization of underlying neural circuitry and a road map for future research. The American journal of psychiatry. 2014; 171:829–843. [PubMed: 24626773]

9. Brandon NJ, Sawa A. Linking neurodevelopmental and synaptic theories of mental illness through DISC1. Nat Rev Neurosci. 2011; 12:707–722. [PubMed: 22095064]

10. Millar JK, et al. Disruption of two novel genes by a translocation co-segregating with schizophrenia. Hum Mol Genet. 2000; 9:1415–1423. [PubMed: 10814723]

11. Mao Y, et al. Disrupted in schizophrenia 1 regulates neuronal progenitor proliferation via modulation of GSK3beta/beta-catenin signaling. Cell. 2009; 136:1017–1031. [PubMed: 19303846]

12. Valvezan AJ, Klein PS. GSK-3 and Wnt Signaling in Neurogenesis and Bipolar Disorder. Front Mol Neurosci. 2012; 5:1. [PubMed: 22319467]

13. O'Brien WT, Klein PS. Validating GSK3 as an in vivo target of lithium action. Biochem Soc Trans. 2009; 37:1133–1138. [PubMed: 19754466]

14. Beaulieu JM, Gainetdinov RR, Caron MG. Akt/GSK3 signaling in the action of psychotropic drugs. Annu Rev Pharmacol Toxicol. 2009; 49:327–347. [PubMed: 18928402]

15. Takahashi K, et al. Induction of pluripotent stem cells from adult human fibroblasts by defined factors. Cell. 2007; 131:861–872. doi:S0092-8674(07)01471-7[pii]10.1016/j.cell.2007.11.019. [PubMed: 18035408]

16. Park IH, et al. Reprogramming of human somatic cells to pluripotency with defined factors. Nature. 2008; 451:141–146. doi:nature06534 [pii]10.1038/nature06534. [PubMed: 18157115]

17. Yu J, et al. Induced pluripotent stem cell lines derived from human somatic cells. Science. 2007; 318:1917–1920. doi:1151526 [pii]10.1126/science.1151526. [PubMed: 18029452]

18. Raya A, et al. Disease-corrected haematopoietic progenitors from Fanconi anaemia induced pluripotent stem cells. Nature. 2009; 460:53–59. doi:nature08129 [pii]10.1038/nature08129. [PubMed: 19483674]

19. Dimos JT, et al. Induced pluripotent stem cells generated from patients with ALS can be differentiated into motor neurons. Science. 2008; 321:1218–1221. doi:1158799 [pii]10.1126/science.1158799. [PubMed: 18669821]

20. Urbach A, Bar-Nur O, Daley GQ, Benvenisty N. Differential modeling of fragile X syndrome by human embryonic stem cells and induced pluripotent stem cells. Cell Stem Cell. 2010; 6:407–411. [PubMed: 20452313]

21. Sheridan SD, et al. Epigenetic characterization of the FMR1 gene and aberrant neurodevelopment in human induced pluripotent stem cell models of fragile X syndrome. PLoS One. 2011; 6:e26203. [pii]. [PubMed: 22022567]

22. Ebert AD, et al. Induced pluripotent stem cells from a spinal muscular atrophy patient. Nature. 2009; 457:277–280. [PubMed: 19098894]

23. Marchetto MC, et al. A model for neural development and treatment of Rett syndrome using human induced pluripotent stem cells. Cell. 2010; 143:527–539. [PubMed: 21074045]

24. Park IH, Daley GQ. Human iPS cell derivation/reprogramming. Curr Protoc Stem Cell Biol. 2009; 4(4A 1)

25. Brennand KJ, et al. Modelling schizophrenia using human induced pluripotent stem cells. Nature. 2011; 473:221–225. [PubMed: 21490598]

26. Brennand KJ, Simone A, Tran N, Gage FH. Modeling psychiatric disorders at the cellular and network levels. Mol Psychiatry. 2012; 17:1239–1253. [PubMed: 22472874]

27. Robicsek O, et al. Abnormal neuronal differentiation and mitochondrial dysfunction in hair follicle-derived induced pluripotent stem cells of schizophrenia patients. Mol Psychiatry. 2013; 18:1067–1076. [PubMed: 23732879]

28. Pedrosa E, et al. Development of patient-specific neurons in schizophrenia using induced pluripotent stem cells. Journal of neurogenetics. 2011; 25:88–103. [PubMed: 21797804]

29. Mostoslavsky G, et al. Efficiency of transduction of highly purified murine hematopoietic stem cells by lentiviral and oncoretroviral vectors under conditions of minimal in vitro manipulation. Molecular therapy : the journal of the American Society of Gene Therapy. 2005; 11:932–940. [PubMed: 15922964]

30. Park IH, Lerou PH, Zhao R, Huo H, Daley GQ. Generation of human-induced pluripotent stem cells. Nat Protoc. 2008; 3:1180–1186. doi:nprot.2008.92 [pii]10.1038/nprot.2008.92. [PubMed: 18600223]

31. Korn JM, et al. Integrated genotype calling and association analysis of SNPs, common copy number polymorphisms and rare CNVs. Nature genetics. 2008; 40:1253–1260. [PubMed: 18776909]

32. ISC. Rare chromosomal deletions and duplications increase risk of schizophrenia. Nature. 2008; 455:237–241. doi:nature07239 [pii]10.1038/nature07239. [PubMed: 18668038]

33. Purcell S, et al. PLINK: a tool set for whole-genome association and population-based linkage analyses. Am J Hum Genet. 2007; 81:559–575. [PubMed: 17701901]

34. Weir BS, Anderson AD, Hepler AB. Genetic relatedness analysis: modern data and new challenges. Nat Rev Genet. 2006; 7:771–780. [PubMed: 16983373]

35. Purcell S, et al. PLINK: a tool set for whole-genome association and population-based linkage analyses. Am J Hum Genet. 2007; 81:559–575. doi:S0002-9297(07)61352-4 [pii]10.1086/519795. [PubMed: 17701901]

36. Yuan SH, et al. Cell-surface marker signatures for the isolation of neural stem cells, glia and neurons derived from human pluripotent stem cells. PLoS One. 2011; 6:e17540. [PubMed: 21407814]

37. Bock C, et al. Reference Maps of human ES and iPS cell variation enable high-throughput characterization of pluripotent cell lines. Cell. 2011; 144:439–452. [PubMed: 21295703]

38. Huber W, von Heydebreck A, Sultmann H, Poustka A, Vingron M. Variance stabilization applied to microarray data calibration and to the quantification of differential expression. Bioinformatics. 2002; 18(Suppl 1):S96–S104. [PubMed: 12169536]

39. Smyth GK. Linear models and empirical bayes methods for assessing differential expression in microarray experiments. Stat Appl Genet Mol Biol. 2004; 3 Article3.

40. Trapnell C, et al. Transcript assembly and quantification by RNA-Seq reveals unannotated transcripts and isoform switching during cell differentiation. Nature biotechnology. 2010; 28:511–515.

41. Pan JQ, et al. AKT kinase activity is required for lithium to modulate mood-related behaviors in mice. Neuropsychopharmacology. 2011; 36:1397–1411. [PubMed: 21389981]

42. Gershon ES, Targum SD, Matthysse S, Bunney WE Jr. Color blindness not closely linked to bipolar illness. Report of a new pedigree series. Archives of general psychiatry. 1979; 36:1423–1430. [PubMed: 316315]

43. Malhotra D, et al. High frequencies of de novo CNVs in bipolar disorder and schizophrenia. Neuron. 2011; 72:951–963. [PubMed: 22196331]

44. Muller FJ, et al. A bioinformatic assay for pluripotency in human cells. Nature methods. 2011; 8:315–317. [PubMed: 21378979]

45. Pan JQ, et al. AKT kinase activity is required for lithium to modulate mood-related behaviors in mice. Neuropsychopharmacology. 2011; 36:1397–1411. [PubMed: 21389981]

46. Koch P, Opitz T, Steinbeck JA, Ladewig J, Brustle O. A rosette-type, self-renewing human ES cell-derived neural stem cell with potential for in vitro instruction and synaptic integration. Proc Natl Acad Sci U S A. 2009; 106:3225–3230. [PubMed: 19218428]

47. Elkabetz Y, et al. Human ES cell-derived neural rosettes reveal a functionally distinct early neural stem cell stage. Genes Dev. 2008; 22:152–165. [PubMed: 18198334]

48. Topark-Ngarm A, et al. CTIP2 associates with the NuRD complex on the promoter of p57KIP2, a newly identified CTIP2 target gene. J Biol Chem. 2006; 281:32272–32283. [PubMed: 16950772]

49. Simon R, et al. A dual function of Bcl11b/Ctip2 in hippocampal neurogenesis. EMBO J. 2012; 31:2922–2936. [PubMed: 22588081]

50. Molyneaux BJ, Arlotta P, Menezes JR, Macklis JD. Neuronal subtype specification in the cerebral cortex. Nat Rev Neurosci. 2007; 8:427–437. [PubMed: 17514196]

51. Folsom TD, Fatemi SH. The involvement of Reelin in neurodevelopmental disorders. Neuropharmacology. 2013; 68:122–135. [PubMed: 22981949]

52. Large-scale genome-wide association analysis of bipolar disorder identifies a new susceptibility locus near ODZ4. Nat Genet. 2011; 43:977–983. [PubMed: 21926972]

53. Green EK, et al. Association at SYNE1 in both bipolar disorder and recurrent major depression. Mol Psychiatry. 2013; 18:614–617. [PubMed: 22565781]

54. Green EK, et al. Replication of bipolar disorder susceptibility alleles and identification of two novel genome-wide significant associations in a new bipolar disorder case-control sample. Mol Psychiatry. 2012

55. Huang J, et al. Cross-disorder genomewide analysis of schizophrenia, bipolar disorder, and depression. Am J Psychiatry. 2010; 167:1254–1263. [PubMed: 20713499]

56. Ripke S, et al. Genome-wide association analysis identifies 13 new risk loci for schizophrenia. Nature genetics. 2013; 45:1150–1159. [PubMed: 23974872]

57. Lage K, et al. A human phenome-interactome network of protein complexes implicated in genetic disorders. Nature biotechnology. 2007; 25:309–316.

58. Zhao WN, et al. A high-throughput screen for Wnt/beta-catenin signaling pathway modulators in human iPSC-derived neural progenitors. Journal of biomolecular screening. 2012; 17:1252–1263. [PubMed: 22923789]

59. Osumi N, Shinohara H, Numayama-Tsuruta K, Maekawa M. Concise review: Pax6 transcription factor contributes to both embryonic and adult neurogenesis as a multifunctional regulator. Stem Cells. 2008; 26:1663–1672. [PubMed: 18467663]

60. Suter DM, Tirefort D, Julien S, Krause KH. A Sox1 to Pax6 switch drives neuroectoderm to radial glia progression during differentiation of mouse embryonic stem cells. Stem Cells. 2009; 27:49–58. [PubMed: 18832594]

61. Israel MA, et al. Probing sporadic and familial Alzheimer's disease using induced pluripotent stem cells. Nature. 2012; 482:216–220. [PubMed: 22278060]

62. Chen HM, DeLong CJ, Bame M, Rajapakse I, Herron TJ, McInnis MG, O'Shea KS. Transcripts involved in calcium signaling and telencephalic neuronal fate are altered in induced pluripotent stem cells from bipolar disorder patients. Transl Psychiatry. 2014; 4:e375. [PubMed: 25116795]

63. Rush AM, et al. Differential modulation of sodium channel Na(v)1.6 by two members of the fibroblast growth factor homologous factor 2 subfamily. Eur J Neurosci. 2006; 23:2551–2562. [PubMed: 16817858]

64. Lou JY, et al. Fibroblast growth factor 14 is an intracellular modulator of voltage-gated sodium channels. J Physiol. 2005; 569:179–193. [PubMed: 16166153]

65. Wittmack EK, et al. Fibroblast growth factor homologous factor 2B: association with Nav1.6 and selective colocalization at nodes of Ranvier of dorsal root axons. J Neurosci. 2004; 24:6765–6775. [PubMed: 15282281]

66. Liu CJ, Dib-Hajj SD, Renganathan M, Cummins TR, Waxman SG. Modulation of the cardiac sodium channel Nav1.5 by fibroblast growth factor homologous factor 1B. J Biol Chem. 2003; 278:1029–1036. [PubMed: 12401812]

67. Yan H, Pablo JL, Pitt GS. FGF14 regulates presynaptic Ca2+ channels and synaptic transmission. Cell Rep. 2013; 4:66–75. [PubMed: 23831029]

68. Xiao M, Bosch MK, Nerbonne JM, Ornitz DM. FGF14 localization and organization of the axon initial segment. Mol Cell Neurosci. 2013; 56:393–403. [PubMed: 23891806]

69. Shavkunov AS, et al. The fibroblast growth factor 14.voltage-gated sodium channel complex is a new target of glycogen synthase kinase 3 (GSK3). J Biol Chem. 2013; 288:19370–19385. [PubMed: 23640885]

70. Group., P. G. C. B. D. W. Large-scale genome-wide association analysis of bipolar disorder identifies a new susceptibility locus near ODZ4. Nature genetics. 2011; 43:977–983. [PubMed: 21926972]

71. Zuko A, et al. Contactins in the neurobiology of autism. European journal of pharmacology. 2013

72. Kerner B, Lambert CG, Muthen BO. Genome-wide association study in bipolar patients stratified by co-morbidity. PLoS One. 2011; 6:e28477. [PubMed: 22205951]

73. Hu QD, et al. F3/contactin acts as a functional ligand for Notch during oligodendrocyte maturation. Cell. 2003; 115:163–175. [PubMed: 14567914]

74. Haggarty SJ, Perlis RH. Translation: Screening for Novel Therapeutics With Disease-Relevant Cell Types Derived from Human Stem Cell Models. Biological psychiatry. 2013
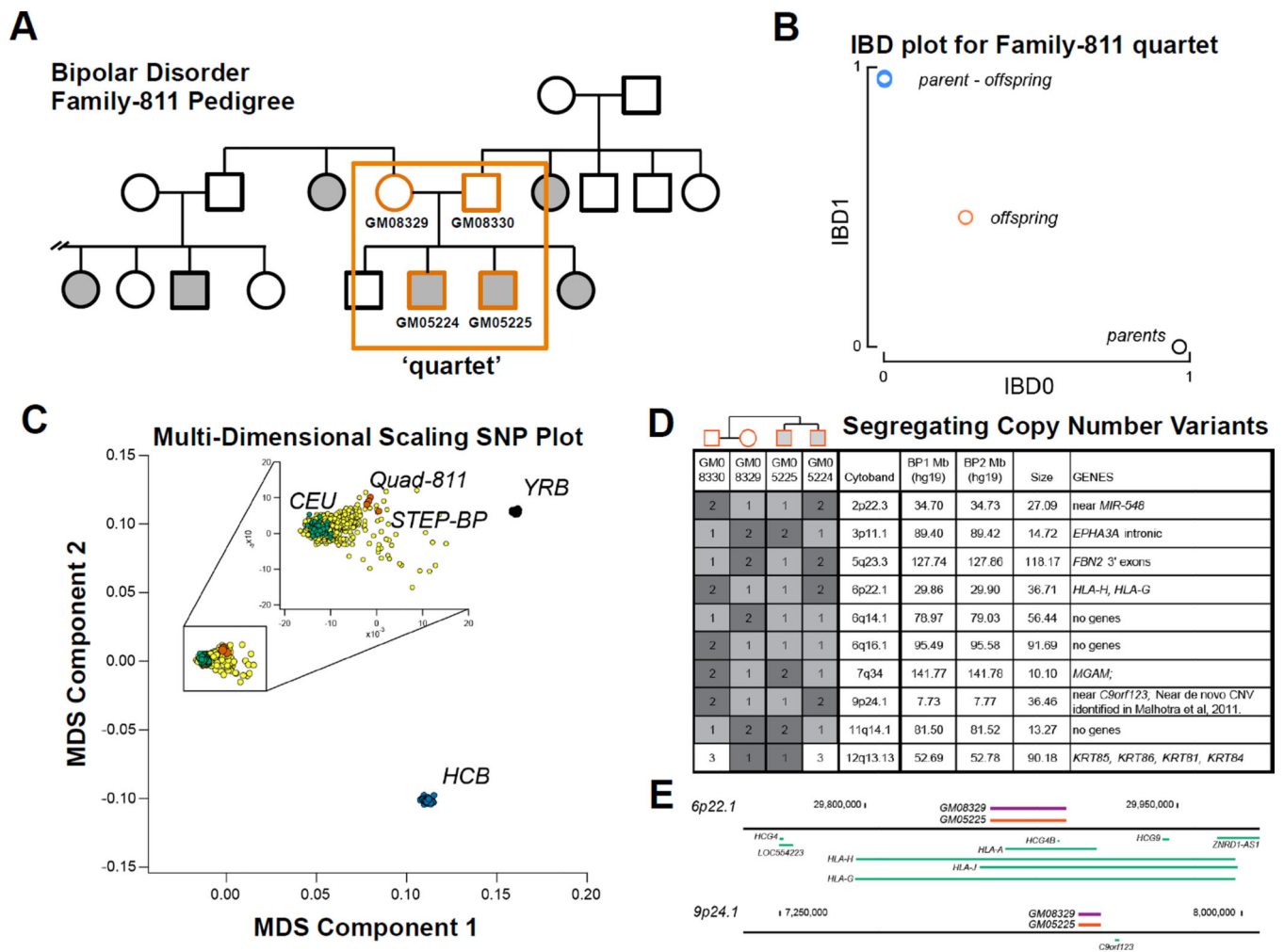
Figure 1. Genomic characterization of Family-811 quartet

(**A**) The pedigree for Family-811 is shown. Males are squares and females are circles. Affected individuals are shaded while unaffected individuals are open. Individuals from the Family-811 quartet studied herein are shown with vermillion squares and circles. The associated Coriell identification numbers are shown below the individuals. GM05224 and GM05225 were both diagnosed with BD type I. (**B**) The familial relationship of these individuals was confirmed using identity-by-descent (IBD) analysis. The IBD1 and IBD2 components were plotted for the parent-parent, parent-offspring and offspring-offspring comparisons. Each of these comparisons agreed with the theoretic prediction of allele sharing for the given familial relationship [(IBD0, IBD1): parent-parent = (1,0), siblings = (1/4,1/2), parent-sibling = (0,1)].[34] (**C**) The multidimensional scaling analysis confirmed that the Family-811 quartet was ethnically related to the CEU Hap Map population and the STEP-BP cohort of individuals used to identify genetically associated bipolar disorder loci. Plotted for comparison are HapMap individuals from Northern and Western Europe (CEU), Yoruba (YRB), and Han Chinese (HCB). (**D**) The complement of CNVs identified in the Family-811 quartet and their segregation, the size, and encompassed genes. Dark grey squares with 2's indicate a homozygous locus while light grey squares indicate a

hemizygous deletion locus, and white squares with a 3 indicate a copy number of 3. The pedigree at the top indicates the familial relationship. (**E**) The orange bars indicate the CNVs as determined by SNP analysis, purple bars indicate CNVs identified by droplet digital PCR and the green bars are genes identified as RefSeq genes.
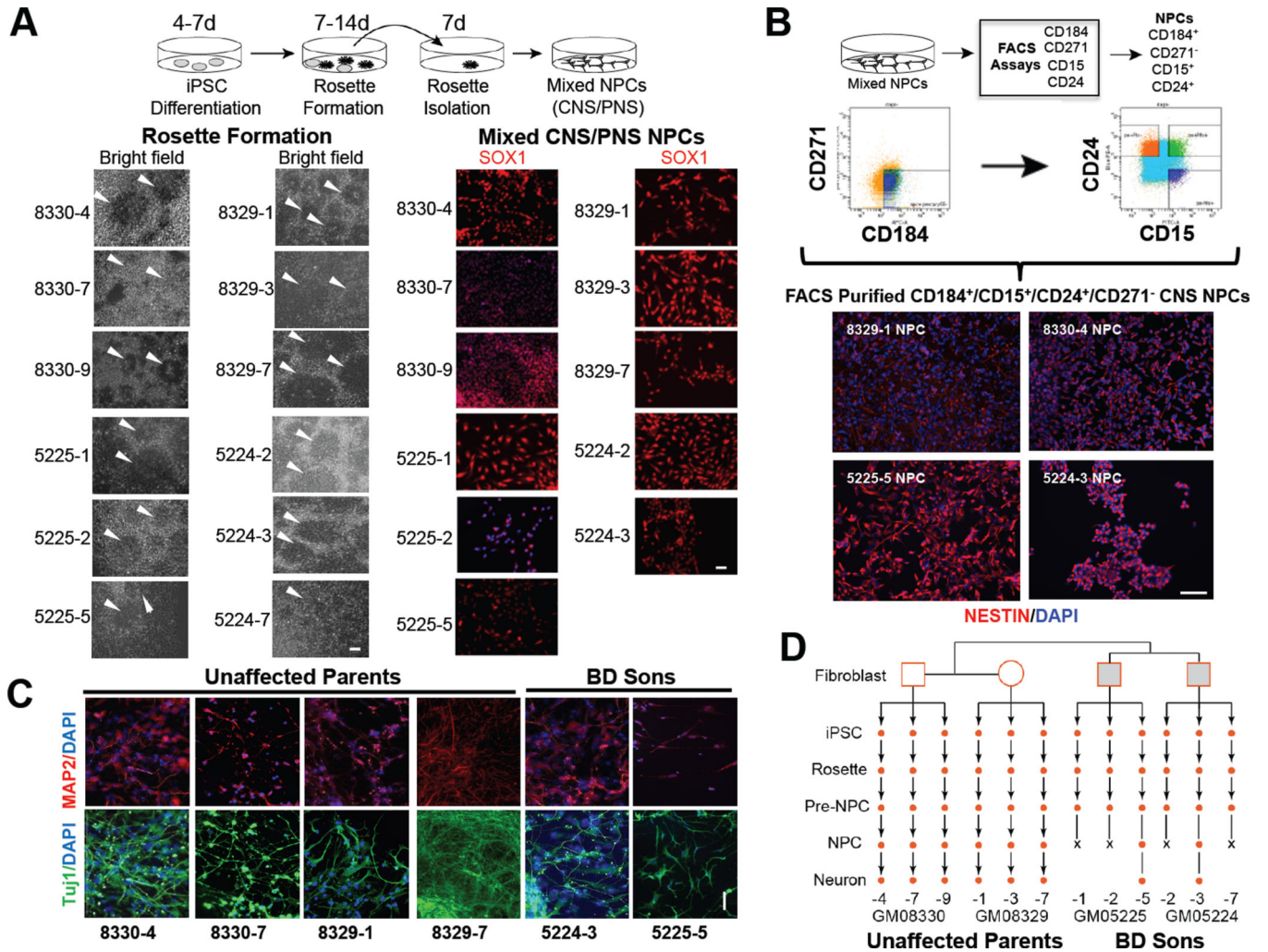
Figure 2. Stepwise neural differentiation of Family-811 quartet iPSCs

(**A**) Schematic of the two-dimensional iPSC neural induction protocol used. Each of the iPSC lines generated from the Family-811 quartet was capable of generating neural rosettes with a characteristic morphology that were manually dissected, passaged and expanded in culture. Each of the iPSC lines was capable of generating SOX1$^+$ cells that could be expanded *in vitro*. (**B**) To derive comparable populations of NPCs, a cell surface signature described by Yuan et al.[36] was used with FACS to isolate CD184$^+$/CD271$^-$/CD24$^+$/CD15$^+$ cells. A representative gating scheme and plot of the events for an experiment is shown. Representative images of CD184$^+$/CD271$^-$/CD24$^+$/CD15$^+$ cells from GM08330, GM08329, GM05225 and GM05224 stained for NESTIN (red) and DAPI (blue) for DNA. (**C**) FACS-purified NPCs from the iPSC lines indicated were differentiated into neurons for six weeks yielding post-mitotic neurons staining for the neuronal markers TuJ1 and MAP2. (**D**) A cell lineage diagram summarizes the cells and cell lines generated from fibroblasts and iPSCs from of each of the individuals in the Family-811 quartet. X's indicate NPC lines that were able to be initally isolated but were unable to be continually expand beyond four or five passages *in vitro* despite mutliple attempts. The scale bar is 100 μm.
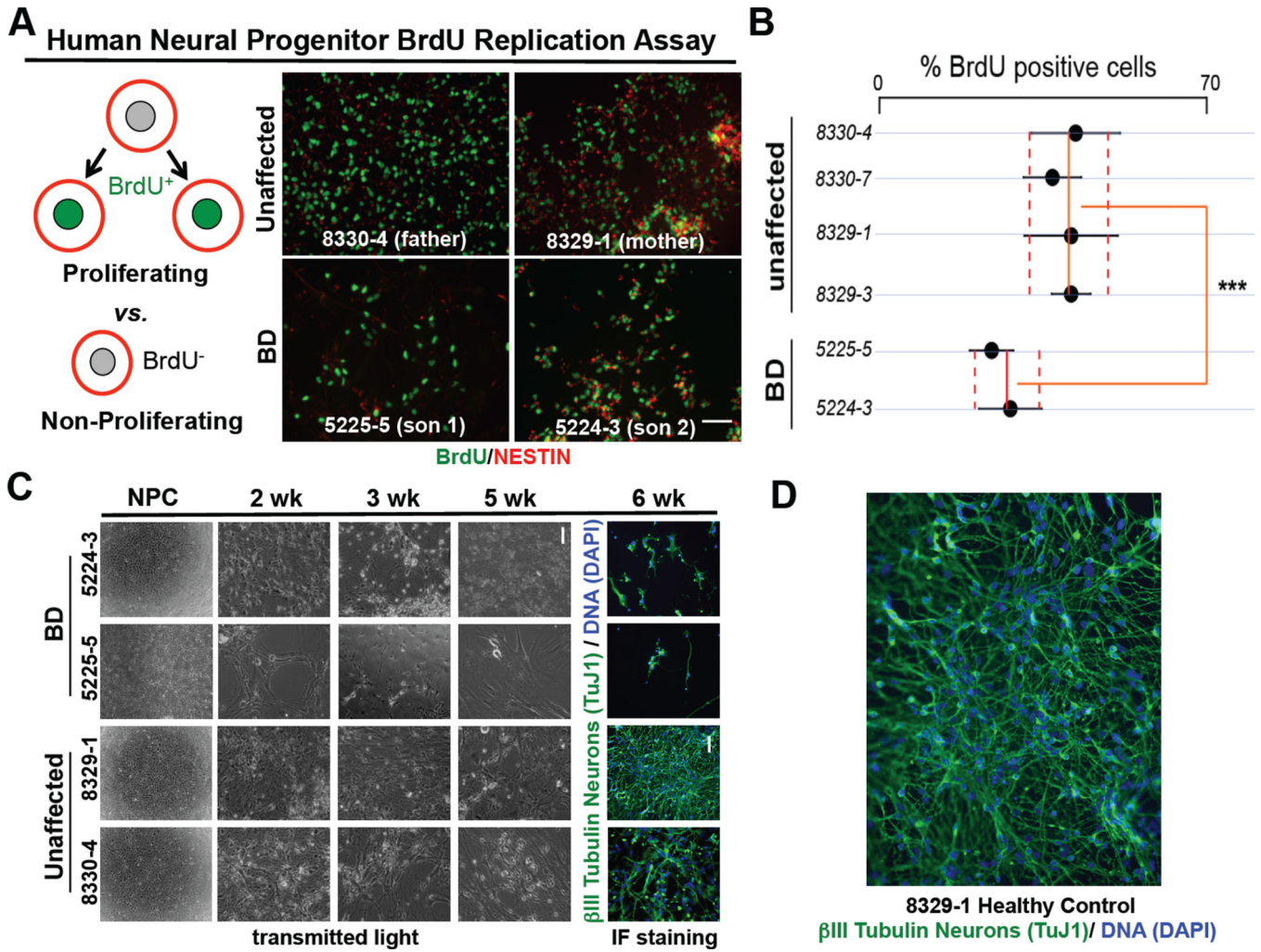
Figure 3. Phenotypic differences of NPCs derived from both BD-patient iPSCs compared to their unaffected parents

(**A**) BrdU incorporation and staining was used to quantify proliferation of the two BD-patient (GM05225, GM05224) and their unaffected parental (GM08330, GM08329) NPC counterparts. (**B**) Bar graph summarizing the percent of cells of the total NESTIN$^+$ cells that incorporated BrdU. The BD-patient NPCs exhibited a significant decrease in BrdU incorporation compared to the mean of the unaffected parents (*** indicates significant, t-test, p=0.001). (**C**) Upon differentiation, BD-patient NPCs (GM05224-3 NPC and GM05225-5 NPC) were found to extend neuritic processes, similar to the unaffected counterparts, but exhibited reduced viability after two weeks of differentiation. In the case of GM05225-5 almost no neurons remained in culture after six weeks. (**D**) Higher magnification of post-mitotic neurons from the parental control NPC line 8329-1 shown in (c). The scale bar is 100 μm. Error bars depict standard deviation of the measurement.
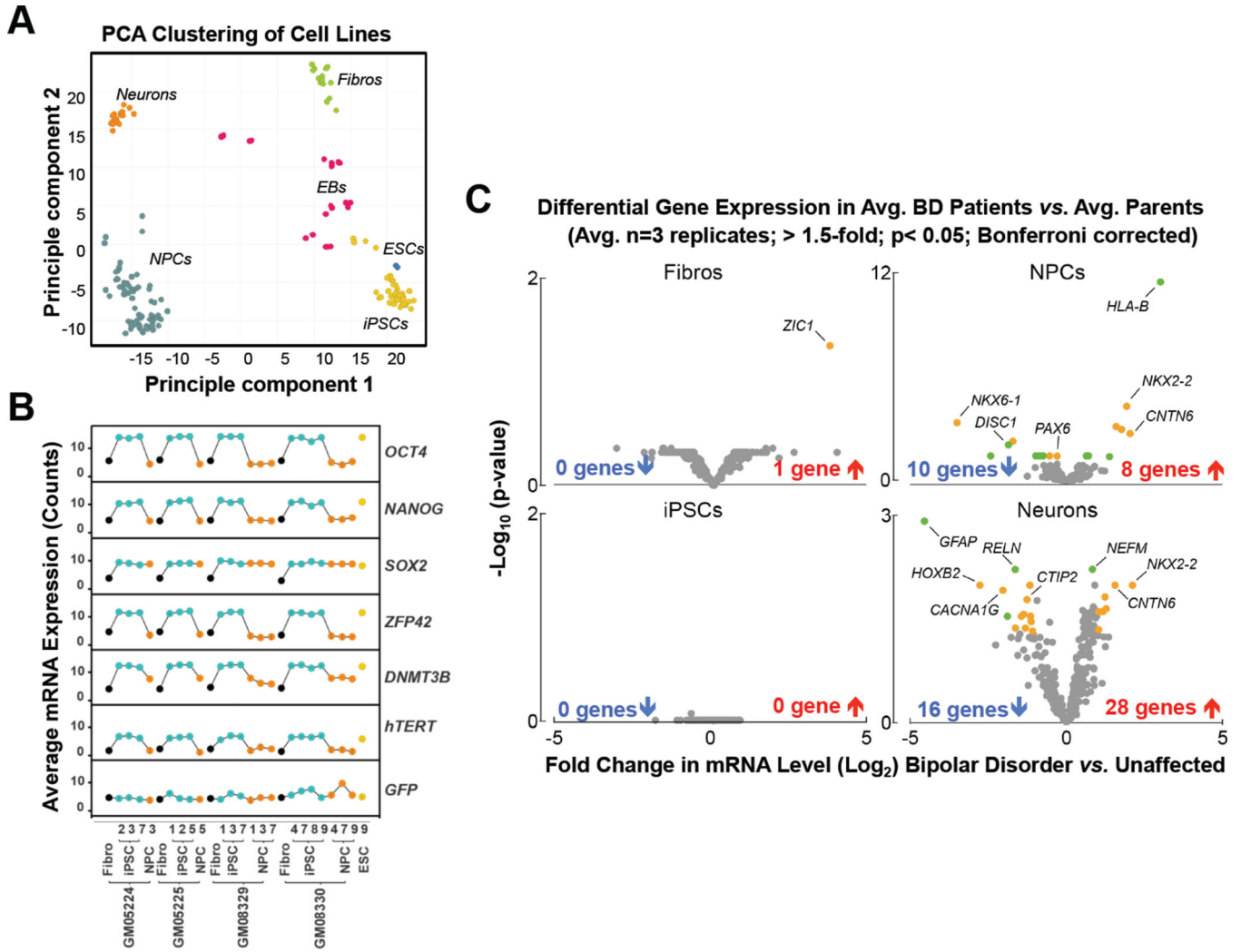
Figure 4. Differential gene expression signature of BD-patient derived NPCs and neurons
(**A**) Principle components analysis (PCA) of a custom PsychGene NanoString profiles from the Family-811 quartet using all 352 of the genes reveals similar grouping of cells by cell type. (**B**) Fibroblasts, iPSCs and NPCs were compared using probes against *OCT4, NANOG, SOX2, ZFP42, DNMT3B, hTERT, MYC, GFP* with total RNA from the human ES cell line H9 shown for comparison. (**C**) Volcano plots of [–$\log_{10}$ (p-value) versus the $\log_2$ (fold change expression)] of all genes (grey dots). Significant, differentially expressed genes (> 1.5-fold comparing BD cells to unaffected cells, moderated t-test p-value < 0.05, Benjamini-Hochberg corrected) were plotted with orange dots with a subset annotated by gene name. Those genes that were also significant when members of the Family-811 quartet were compared based on sex (i.e. GM08329 versus GM8330, GM05225 and GM05225) were colored green. Gene expression differences were found to be enriched in the BD-patient NPCs and neuronal populations. Each dot represents a gene expression assay (n=3) for the cell type indicated. Error bars depict standard deviation of the measurement.
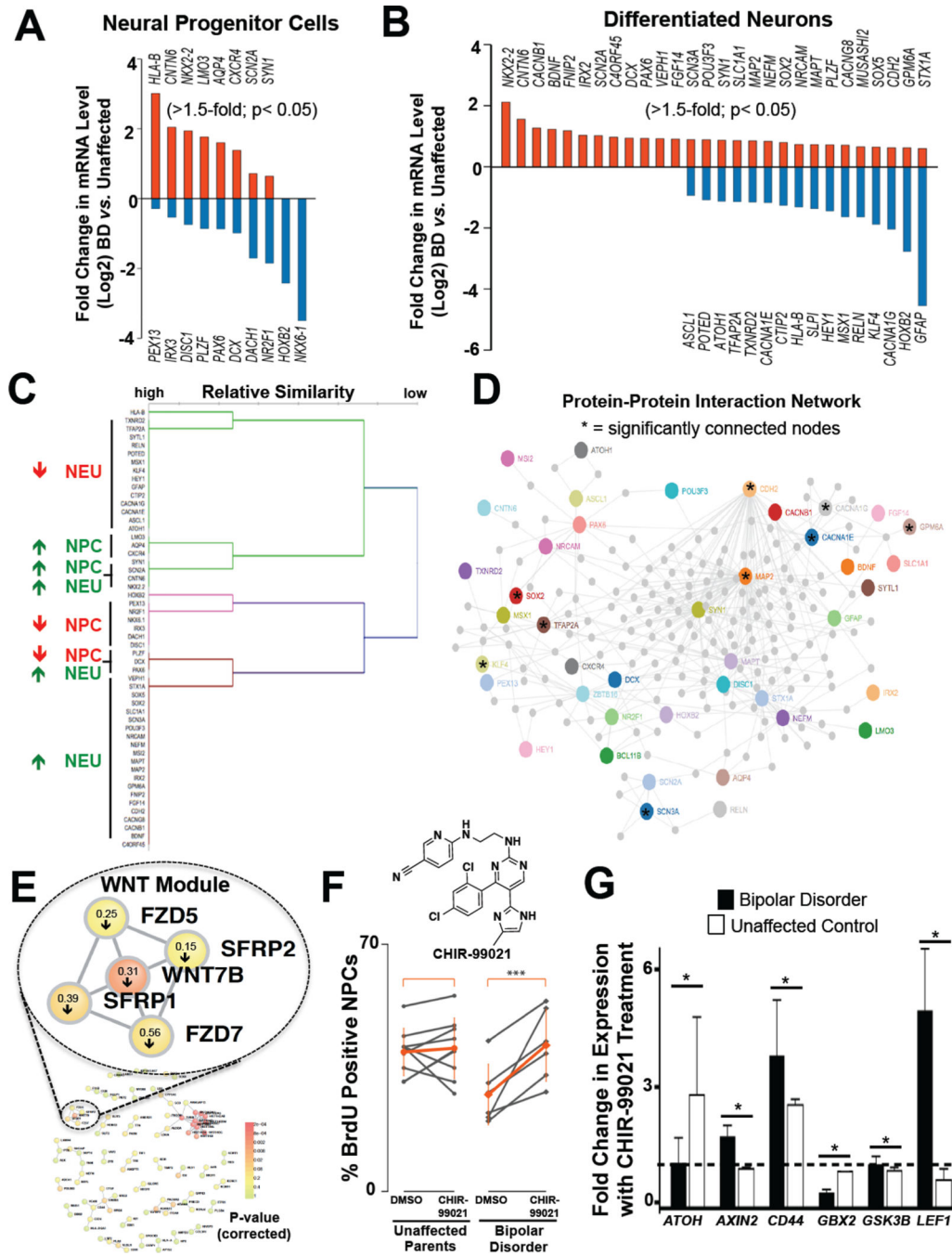
Figure 5. Gene expression differences in the BD-patient iPSC neural derivatives

Differential gene expression (>1.5 fold at a significance of $p<0.05$ calculated using a moderated t-test and corrected using the Benjamini-Hochberg test) in (**A**) BD-patient CXCR4^{+} NPCs and (**B**) in BD-patient neurons relative to the unaffected parental cells. Genes with increased expression are shown in red; genes with deceased expression are shown in blue. (**C**) Agglomerative hierarchical clustering of the 53 differentially expressed genes between BD-patient CXCR4^{+} NPCs and differentiated neurons using a weighted pair-group average method and a Pearson correlation coefficient as the similarity metric. (**D**)

DAPPLE protein-protein interaction network amongst differentially expressed genes form the PsychGene NanoString profiles between BD-patient CXCR4$^+$ NPCs and differentiated neurons demonstrating a statistically significant high degree of interconnectivity for specific nodes (marked with *) and globally. (**E**) WNT module within the DAPPLE protein-protein interaction network amongst differentially expressed genes from the global RNA-seq analysis composed of WNT7B and four additional input seeds amongst the direct interactions all of which were downregulated (levels indicated with arrow) in the BD-patient CXCR4$^+$ NPCs compared to the parental control CXCR4$^+$ NPCs.

(**F**) Rescue of DNA synthesis deficits in the BD-patient NPCs with WNT pathway activation. BrdU incorporation data with pairs of DMSO and CHIR-99021 treated cell lines represented with a symbol connected by a bar. Cell were treated for 16 hours with either DMSO (vehicle) or CHIR-99021 (5 μM), labeled with BrdU, fixed, and stained to detect BrdU and NESTIN. Proliferation was measured by counting BrdU labeled nuclei and quantifying percent of NESTIN$^+$ cells labeled with BrdU. The orange symbol and bars represent averages of the BrdU incorporation experiments in the presence of either DMSO or CHIR-99021. The proliferation defect observed in the BD-patient CXCR4$^+$ NPCs was significantly (pair-wise t-test, p=0.02) decreased with CHIR-99021 treatment while the proliferation of the unaffected parental CXCR4$^+$ NPCs was not changed. (**G**) CHIR-99021 treatment (16 hours, 5 μM) alters the expression of a subset of WNT pathway responsive genes in the BD-patient CXCR4$^+$ NPCs measured using the PsychGene NanoString probe set. Several genes were upregulated (> 1.5-fold; p-value <0.05 Benjamini-Hochberg corrected) in the BD-patient NPC cell line, including *CD44, LEF1, AXIN2* and down regulated (*GBX2*), while others were only responsive in the parental control lines (*ATOH, GSK3B*) unaffected. Error bars depict standard deviation of the measurement.

Table 1

Gene Ontology (GO) category analysis of global RNA-seq data comparing bipolar disorder CXCR4+ NPCs to control CXCR4+ NPCs.

GO Term Category	Term	Count	% of Gene Set	Fold Enrichment	P-Value (corrected)
Biological Process	GO:0030182~neuron differentiation	36	8.4	3.4	1.05E-06
	GO:0048666~neuron development	28	6.5	3.4	2.97E-05
	GO:0031175~neuron projection development	22	5.1	3.5	4.60E-04
	GO:0048812~neuron projection morphogenesis	19	4.4	3.7	0.0015
	GO:0048858~cell projection morphogenesis	20	4.6	3.4	0.0024
	GO:0048667~cell morphogenesis involved in neuron differentiation	18	4.2	3.5	0.003
	GO:0032990~cell part morphogenesis	20	4.6	3.2	0.0031
	GO:0007409~axonogenesis	17	3.9	3.6	0.0035
	GO:0000904~cell morphogenesis involved in differentiation	19	4.4	3.2	0.0044
	GO:0031099~regeneration	10	2.3	6.0	0.0054
	GO:0016337~cell-cell adhesion	20	4.6	3.0	0.0055
	GO:0030334~regulation of cell migration	15	3.5	3.6	0.0075
	GO:0040012~regulation of locomotion	16	3.7	3.4	0.0076
	GO:0051270~regulation of cell motion	16	3.7	3.4	0.0077
	GO:0009991~response to extracellular stimulus	17	3.9	3.2	0.0093
	GO:0021700~developmental maturation	11	2.6	4.5	0.016
	GO:0043062~extracellular structure organization	14	3.2	3.5	0.015
	GO:0048469~cell maturation	9	2.1	4.9	0.038
Cellular Compartment	GO:0031012~extracellular matrix	28	6.5	3.4	1.90E-05
	GO:0005578~proteinaceous extracellular matrix	25	5.8	3.3	1.10E-04
	GO:0044420~extracellular matrix part	12	2.8	4.3	0.0042
	GO:0000786~nucleosome	9	2.1	5.9	0.004
	GO:0005604~basement membrane	9	2.1	4.8	0.014
	GO:0032993~protein-DNA complex	9	2.1	4.4	0.022
Molecular Function	GO:0005509~calcium ion binding	42	9.7	1.9	0.056